

DEVELOPING AN ELECTROSTATIC DISCHARGE POLYAMIDE 6
NANOCOMPOSITE FOR 3D PRINTING

by

Oluwasola Kofoworola Arigbabowo, B.Sc., M.Sc.

A thesis submitted to the Graduate Council of
Texas State University in partial fulfillment
of the requirements for the degree of
Master of Science
with a Major in Engineering
August 2020

Committee Members:

Jitendra S. Tate, Chair

Namwon Kim

Gary Beall

COPYRIGHT

by

Oluwasola Kofoworola Arigbabowo

2020

FAIR USE AND AUTHOR'S PERMISSION STATEMENT

Fair Use

This work is protected by the Copyright Laws of the United States (Public Law 94-553, section 107). Consistent with fair use as defined in the Copyright Laws, brief quotations from this material are allowed with proper acknowledgement. Use of this material for financial gain without the author's express written permission is not allowed.

Duplication Permission

As the copyright holder of this work I, Oluwasola Kofoworola Arigbabowo, authorize duplication of this work, in whole or in part, for educational or scholarly purposes only.

ACKNOWLEDGEMENTS

My profound gratitude and indebtedness go to my thesis supervisor, Dr Jitendra S. Tate for his mentorship during this research work. I appreciate the efforts of members of my thesis committee - Dr. Kim Namwon and Dr. Gary Beall for their technical advice towards this thesis. I am grateful to my graduate advisor, Dr. Vishu Viswanathan for his guidance throughout my M.Sc. Program. Also, to the Administrative of Ingram School of Engineering, I say thank you for offering me a support in form of a GIA throughout my program and God will reward you genuinely for all the kind gesture.

I wish to express my warmth heart appreciation to my parents; Dr. and Chief (Mrs.) A. S. Arigbabowo and to my siblings; Oluwaseyi, Fehintola and Adenike for their moral, spiritual, and physical supports. Also, for being my benefactor and guide all through my program.

Many thanks go to every member of Advance Composite Research team for their assistance in terms of technical support during the experimentation process, may God reward you. Also, to my friends and colleagues, particularly Zeasuchia Tate for their moral support and assistance.

Finally, my endless gratitude goes to Almighty God; the One who is always there for me, for His love, care, mercy, guidance and for sparing my life till this moment and making this program a success.

TABLE OF CONTENTS

	Page
ACKNOWLEDGEMENTS	iv
LIST OF TABLES	vii
LIST OF FIGURES	viii
LIST OF ABBREVIATIONS	x
ABSTRACT	xi
CHAPTER	
1. INTRODUCTION	1
1.1 Background Information	1
1.1.1 Motivation of study	5
1.1.2 Target applications	6
1.1.3 Literature review	6
1.1.4 Objectives of study	9
1.2 Materials System	10
1.2.1 Polyamide 6 (Nylon 645)	10
1.2.2 Carbon nanofibers (PR-24-XT-LHT)	10
1.3 Manufacturing	11
1.3.1 Melt compounding	11
1.3.2 3D printing	12
2. EXPERIMENTATION	14
2.1 Materials Preparation	14
2.2 Twin Screw Compounding	15
2.2.1 Dispersion of carbon nanofiber	16
2.3 Fused Deposition Modelling	18
2.3.1 Printing parameters	19
3. MATERIALS CHARACTERIZATION	20
3.1 Microstructural Investigation	20

3.2 Mechanical Testing	21
3.2.1 Tensile testing	21
3.2.2 Flexure testing.....	22
3.3 Electrical Testing	22
3.4 Thermal Analysis	23
4. RESULTS AND DISCUSSION	25
4.1 Microstructural Evaluation	25
4.2 Mechanical Properties.....	26
4.3 Volume Resistivity	30
4.4 Thermogravimetry	32
4.5 Differential Scanning Calorimetry	35
4.6 Dynamic Mechanical Analysis	38
5. CONCLUSION AND RECOMMENDATION.....	41
5.1 Conclusion	41
5.2 Recommendation	42
APPENDIX SECTION.....	43
REFERENCES	46

LIST OF TABLES

Table	Page
1. Characteristics of Aliphatic Polyamides (Nylons)	2
2. Material Properties of Carbon Conductive Fillers	3
3. 3D Printing Parameters of PA6/CNF Nanocomposites	19
4. Mechanical Properties Data	26
5. Volume Resistivity Values	31
6. Thermogravimetric Analysis	33
7. DSC Thermal Transitions	35

LIST OF FIGURES

Figure	Page
1. (a) Electrical Conductivity of Conducting Polymers (b) Polymers Electrical Resistivity Ranges.....	5
2. Percolation Phenomenom in Conducting Composites.....	8
3. (a) Prior debulked CNF (b) “XT” improved debulked CNF	11
4. Melt Compounding Process.....	12
5. Fused Deposition Modelling 3D Printing	13
6. (a) Nylon 645 pellets (b) Vacuum Dryer	15
7. (a) Twin Screw Extruder (11mm diameter) (b) Twin Screws Elements	16
8. (a) Filabot Spooler (b) Control Screen.....	17
9. Twin-screw Extrusion Parameters	17
10. 3D printing (a) Enclosure Box (b) of Tensile Samples(c) of ESD Samples	18
11. Field Emission Scanning Electron Microscope (FE SEM).....	20
12. Tension test of 3D Printed PA6/CNF Nanocomposites.....	21
13. (a) Keithely Megohmmeter Setup (b) Effective Circular Electrode.....	23
14. (a) Simultaneous Differential Thermogravimetry-SDT 650 (b) Dynamic Mechanical Analyzer-DMA 2980.....	24
15. SEM images of (a) 3wt% (b) 5wt% 3D Printed PA 6/CNF Nanocomposites.....	25
16. Tensile and Flexural Strength of 3D Printed PA6/CNF Nanocomposites.....	27
17. Tensile and Flexural Modulus of 3D Printed PA6/CNF Nanocomposites	28

18. % Elongation and Toughness of 3D Printed PA6/CNF Nanocomposites	29
19. Tensile stress vs Axial strain of 3D Printed PA6/CNF Nanocomposites	30
20. Volume Resistivity of 3D Printed PA6/CNF Nanocomposite.....	32
21. TGA/DTGA Curve of PA6/CNF Nanocomposites	34
22. DSC Scan of PA6/CNF Nanocomposites	36
23. DMA Thermograms of Storage Modulus – Temperature Profile.....	39
24. DMA Thermograms of Loss Modulus – Temperature Profile	39
25. DMA Thermograms of Tan Delta – Temperature Profile	40

LIST OF ABBREVIATIONS

Abbreviation	Description
PA 6	Polyamide 6
CNF	Carbon Nanofiber
FDM	Fused Deposition Modelling
ESD	Electrostatic Discharge
TSE	Twin Screw Extruder
SEM	Scanning Electron Microscope
SDT	Simultaneous Differential Thermogravimetry
TGA	Thermogravimetric Analysis
DTGA	Differential Thermogravimetric Analysis
DSC	Differential Scanning Calorimetry
DMA	Dynamic Mechanical Analyzer

ABSTRACT

Polyamide 6 (PA 6) is an engineering thermoplastic ideal for 3D printing via fused deposition modelling (FDM) and could serve as potential replacement for conventional FDM polymers like acrylonitrile-butadiene-styrene (ABS) and Polylactic acid (PLA). The addition of nanofillers at low concentrations can be a promising advancement in fabricating PA 6 based nanocomposites filaments for FDM process thereby expanding its use in applications demanding for good electrical properties like electrostatic dissipation (ESD). While creating an electrically conductive path to improve the ESD capability, it is imperative to sustain the structural integrity of the nanocomposites. Hence, the primary goal of this research was to develop a viable PA6 nanocomposites filament for 3D printing in potential electrostatic discharge applications. 3 and 5 wt.% loadings of Carbon Nanofiber (CNF) were compounded with PA6 using co-rotating twin screw extruder to produce 1.75mm diameter monofilaments for fused deposition modelling (FDM). The morphology of the compounded nanocomposites was investigated using Scanning Electron Microscope and test samples were printed using commercial-off-the-shelf (COTS), Lulzbot TAZ 6 FDM printer. Mechanical, electrical, and thermal characterization were carried out according to their respective ASTM standard. The tensile properties were enhanced by 3wt% addition of CNF, but no observable improvement in tensile modulus at 5wt%. The flexural strength and modulus increase with increasing addition of CNF. The thermal properties of the nanocomposites were sustained with incorporation of CNF with no major deterioration in thermal stability

and a higher degree of crystallinity was observed at both CNF loading levels. The electrical resistivity of the insulative PA6 matrix was reduced to order of 10^{-11} Ω -cm and 10^{12} Ω -cm by 3wt% and 5wt% CNF addition respectively, which seems promising for manufacturing of static discharge products. The modification of the PA 6 matrix with inclusion of CNF has shown high potential of developing a multifunctional PA6 nanocomposite filament for 3D printing and this was significant at 3wt% CNF addition which possess an excellent combination of mechanical, electrical, and thermal properties.

Key Words: Polyamide 6, Carbon Nanofiber-CNF, Twin Screw Extrusion -TSE, Fused Deposition Modelling- FDM, Electrostatic Dissipation (ESD).

1. INTRODUCTION

1.1 Background Information

Polyamide 6 (PA 6) belongs to high performing engineering thermoplastics generally known as Nylons. Depending on the number of carbon atoms in their repeating unit, they can be majorly categorized as presented in Table 1. They are semi crystalline in nature and possess good balance of material properties and as a result, they have been widely utilized in automotive, electronics and sports related applications. The presence of the amide bonds presents in their polymer chain makes them susceptible to moisture. Despite the negative impact of their moisture sensitivity on electrical properties and dimensional stability, the absorbed moisture could act as a plasticizer and consequently improves their impact and fatigue resistance. They are viable material choice in 3D printing and based on the performance to cost ratio, PA 6 has been widely considered in manufacturing high end engineering products. PA 6 possess a high manufacturing flexibility and they can be modified to form novel nanocomposites

PA 6 nanocomposites is a functional material that exploits the unique properties of specific nanoparticles. It is an engineering material that can be tailored to a targeted application. In enhancing the electrical performance in PA 6 nanocomposites, the conductive nanoparticles typically employed are carbon fillers, such as carbon black, carbon nanotubes, carbon nanofibers and nanographene platelets. These class of nanoparticles exhibits good mechanical, thermal properties, fire retardancy in addition to their electrical performance as enumerated in Table 1. Using a wide range of dispersion techniques such as high shear mixer, ultrasonication and twin-screw extruder, they can be dispersed in PA 6 matrix, achieving a considerable low percolation threshold [1].

Table 1: Characteristics of Aliphatic Polyamides (Nylons)

Characteristics	PA 6	PA 6,6	PA 11	PA 12
Monomers	Caprolactam	Hexamethylene diamine & adipic acid	11-amino undecanoic acid	Lauro lactam
Polymerization	Open ring	Polycondensation	Bio based	Open ring
Properties				
Strength	High	High	Low	Low
Stiffness	High	High	Low	Low
Impact strength	High	High	Low	Low
Fatigue resistance	High	High	Very High	Very High
Dimensional stability	High	High	High	High
Chemical resistance	Low	Low	High	Very high
Cost effectiveness	Very Low	Low	High	High
%Moisture absorption rate (RH 50% at 23 C)	2.7	2.5	0.8	0.7
3DPrinting technique	FDM	FDM	SLS/MJF	SLS/MJF
Applications	Air intake manifolds, Fuel tank caps, Electrical switches	Gear wheels, Radiator caps, Hammer heads	Sport shoe soles, Spray painting hose,	Trailer brake hoses, Fuel lines, Air ducts

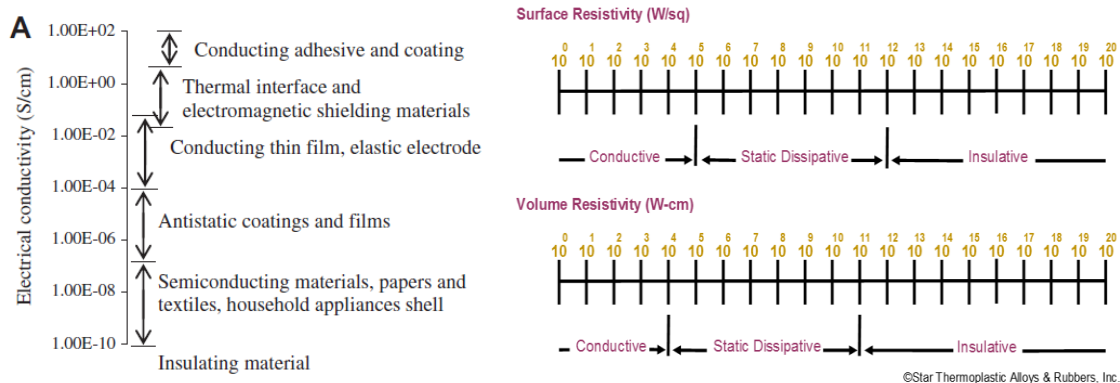
Polyamide 6 nanocomposites is a functional material that exploits the unique properties of specific nanoparticles. It is an engineering material that can be produced and tailored to a targeted application. In enhancing the electrical performance in Polyamide 6 nanocomposites, the common conductive nanoparticles employed are carbon fillers, typically carbon black, carbon nanotubes, carbon nanofibers and nanographene platelets. These class of nanoparticles exhibits good mechanical, thermal properties, fire retardancy properties in addition to their electrical performance as enumerated in Table 1. Using a wide range of dispersion techniques such as high shear mixer, ultrasonication and twin-screw extruder, they can be dispersed in polyamide 6 matrix, achieving a considerable low percolation threshold [1].

Table 2: Material Properties of Carbon Conductive Fillers

Property	Carbon Black	Carbon nanotubes	Graphene nanoplatelets	Carbon nanofibers
Physical structure	Powdery	Cylindrical	Platelets	Cylindrical
Dimension/Size		1nm X 100nm	1nm X 100nm	20nm X 100nm
Density (g/cm ³)	2.26	1.2 –1.4	~2.0	1.8-2.1
Tensile Strength (GPa)	4.8	3-40	~ (10-20)	3-7 GPa
Tensile Modulus (TPa)	4.1	0.6-1	~1.0 TPa	3-7 GPa
Thermal Cond.	~114	3000 W/m·K	3000W/mk	20-2000 W/m·K
Electrical resistivity	~10 ⁻⁶ Ω cm	~ 50 x 10 ⁻⁶ Ω cm	~ 50 x 10 ⁻⁶ Ω cm	5-100 x 10 ⁻³ Ω cm
Coefficient of Thermal Expansion	0.6 x 10 ⁻⁶	-1 x 10 ⁻⁶	-1 x 10 ⁻⁶	-1 x 10 ⁻⁶

The percolation threshold is the minimum quantity of the nanoparticles required to form a conductive path within the Polyamide 6 matrix. The resulting conductive polyamide 6 nanocomposite has been attractive to electromagnetic shielding (EMI) and electrostatic discharge applications (ESD). Other applications of conductive nanocomposites are presented in Figure 1 [1].

Electrostatic discharge is a high voltage electrical activity that arises from the release of electrical energy due to static electricity or electrostatic induction [2]. ESD capability can be quantified by the electrical resistivity measurements, as presented in Fig 1. In combating the risk of ESD, electrically conductive and static dissipative polymers have been identified to be able to lastingly control and dissipate electrostatic charges [3]. The electrical resistivity of this class of polymers can be characterized by either evaluating their surface or volume resistivity. The surface resistivity measures the polymer's resistance to leakage current along its surface while the resistance posed to leakage current through its body represent the volume resistivity. The electrical resistivity values are dependent on the applied voltage, electrification time and environmental factors and these factors should be monitored. Plastics being intrinsically insulative, research effort has been projected modification of the matrix to develop novel static dissipative polymer nanocomposite for emerging manufacturing technique like 3D printing. While improving the static dissipative ability of polymers, it is imperative to sustain the structural integrity such as mechanical properties, thermal stability, and flame retardancy, thereby increase its multifunctional ability and increase the potential engineering application.



(a)

(b)

Figure 1 (a) Electrical Conductivity of Conducting Polymers[1] (b) Polymers Electrical Resistivity Ranges[4]

1.1.1 Motivation of study

Polyamide 6 (PA 6) is one of the most widely utilized thermoplastics in manufacturing. It has been considered suitable material choice in producing end use functional parts via 3D printing[5] - creating parts layer by layer from a 3D geometrical model as opposed to conventional subtractive manufacturing techniques. Furthermore, it affords advantages of overall cost efficiency, flexibility, and manufacturability of custom polymers without jeopardizing their intrinsic properties. Aside from being an ideal 3D printing material, easy modification of Polyamide 6 has made them practical for vast uses and promising applications[6].

Despite their great potential in offering excellent thermal and mechanical properties, the lack of mobile electron carriers, typical of polymeric materials, has been perceived as a major drawback in expanding its use in applications demanding for good electrical properties such as electrostatic discharge. Conductive fillers such as metal powders and carbon nanofillers will make polymers less resistive to electricity, thereby qualify them for ESD applications. However, metal fillers increase density thereby

jeopardizing the intrinsic nature of weight advantage in polymers. Although carbon nanofillers are Carbon black deteriorates the mechanical properties.

Therefore, it is hypothesized that Carbon nanofibers, CNT, and GNP are viable options as small loading levels without much increase in the density, will reduce electrical resistivity without reduction in mechanical properties.

1.1.2 Target applications

Polyamide 6 is a high-performance engineering plastic and incorporation of conductive carbon fillers in the polyamide could lead to light weight multifunctional materials that are electrostatically dissipative. Such materials may have many applications in the electronics, aerospace and automotive industries, especially in composite structures to prevent deleterious effects of ESD and lightning strikes. Polyamide 6 nanocomposite can be used in prototyping and end use engineering applications such as manufacturing of static products in electronics like conductive bin, integrated circuit trays and conveyer plate of semiconductors. In addition, certain part of aircraft fuselage like access panel and air ventilation duct. In automotive, it is a material choice for tail gate handles and fuel tank caps.

1.1.3 Literature review

Polymers are considered the most plausible choice employed in 3D printing due to their ease of adoption to different 3D printing processes. They are predominantly found in the form of thermoplastic filaments in the case of Fused Deposition Modelling (FDM) [7]. The conventional polymers used in FDM are acrylonitrile-butadiene-styrene (ABS) and Polylactic acid (PLA), however they are not devoid of certain shortcomings. ABS possess good mechanical properties but emits unpleasant odor when melted whereas

PLA is ecofriendly but has poor mechanical properties [8]. The addition of a second phase in form of nanoparticles reinforcement could be a promising advancement in 3D printing.

According to T.D. Ngo *et al.* (2017), nanoparticles are emerging materials capable of improving the mechanical and electrical properties of conventional thermoplastic filaments. These nanoparticles could be introduced via premixing into the host matrix, yielding a homogeneous nanocomposite product for engineering applications. Postigliopone *et al.* (2015) successfully developed a polymer nanocomposite of PLA blended with multi walled carbon nanotubes via a low-cost liquid deposition modelling (LDM) 3D printing technique. Furthermore, vapor grown carbon fiber has been incorporated as a nanofiller in ABS to strengthen the matrix, thereby resulting into a quality nanocomposite with a uniform distribution and minimal porosity viable for FDM 3D printing [9]. In developing host matrices with better mechanical properties, Nylon 6 has been considered as a technological alternative to ABS for 3D printing [10].

Boparai (2016) studied Nylon 6 based nanocomposites as a potential FDM filament material. Aside from being an ideal 3D printing material, easy modification of PA 6 has made them practical for vast uses and promising applications [6]. Despite their great potential in offering excellent thermal and mechanical properties, the lack of mobile electron carriers, typical of polymeric materials, has been a major drawback in expanding its use in applications demanding for good electrical properties. This can be addressed by creating a three-dimensional low resistance network for electron flow and modifying the Polyamide 6 matrix with conductive nanoparticles could be considered a plausible solution for electromagnetic shielding (EMI) and electrostatic discharge (ESD) concerns.

Carbon fillers such as carbon black, carbon nanotubes (CNT), nanographene platelets (NGP) and carbon nanofiber (CNF) have been identified to be viable in this regard and their incorporations into PA 6 matrix could results in a novel type Polyamide 6 nanocomposites.

Bauhofer (2009) reported that the PA6 percolation threshold could be achieved at loading levels as low as 2.5wt.% or higher CNT loading. In addition, Zonder *et al.* (2011) affirmed that PA 12 can better disperse CNT due to its polar nature and electrical and rheological percolation was achieved around 1.4wt% CNT. This ability has been attributed to the large aspect ratio (length-diameter) typical of fillers as carbon nanotubes and carbon nanofibers fillers[11]. The percolation threshold, as illustrated in Figure 1, is the minimum quantity of filler required to form a conductive path within the polymer. In the work of Gaikwad *et al.* (2013), where NGP was successfully dispersed in PA11 using co-rotating twin-screw extruder, the percolation threshold was achieved at 7wt% NGP. They emphasized that manufacturing method of composites plays important role in percolation threshold as it affects orientation, dispersion, aspect ratio of filler and interparticle spacing within the polymer matrix [12].

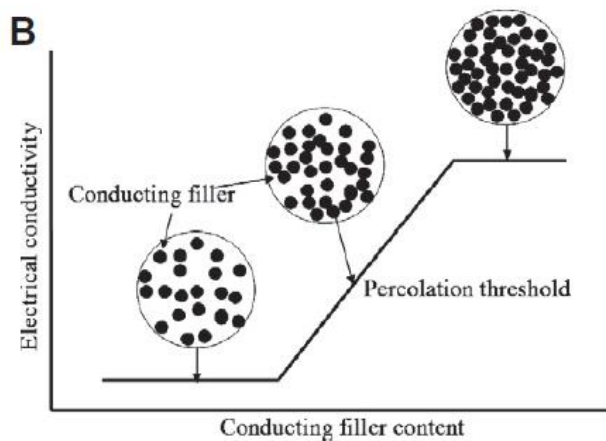


Figure 2: Percolation Phenomenon in Conducting Composites [1]

Carbon nanofibers has been identified to enhance the stiffening of thermoplastics matrix. Alongside, it improves the thermal and thermo-oxidative stabilities of the matrix, and dispersion of CNF was reported to have acted as nucleation sites, thereby leading to formation of new crystalline domains [13, 14]. According to Goodridge (2011), the improvement in tensile properties obtained via laser sintering of PA12/Carbon Nanofiber (CNF) composites was attributed to the high aspect ratio of the nanofibers. Aspect ratio is the proportional ratio of length to diameter of the fibers. The diameter of CNF ranges between 20-200nm which are quite larger than that of carbon nanotubes (2-100 nm) and their length can be more than a micron, resulting into high aspect ratio of CNF and CNT > 100 [15-17]. In addition to the low density and high aspect ratio of CNF, it has been considered more economical than CNT in terms of manufacturability and monetary cost [17], thereby proving more viable in developing advance nanocomposites. Hence, this research was aimed to develop a carbon nanofiber-polyamide 6 nanocomposite with good combination of electrical properties and structural integrity that would be viable for 3D printing of high-end engineering products for use in Electrostatic Discharge Applications.

1.1.4 Objectives of study

The overall goal of this research efforts is to obtain a viable 3D printing structural material for ESD application. The specific objectives are to

1. Effectively compound the nanofillers with polyamide 6 to produce quality filaments for 3D printing.
2. Evaluate the dispersion of GNP and CNF in PA 6 via SEM.
3. Characterize the mechanical, thermal, and electrical performance of the developed material.

4. Correlate the materials performance with the dispersion state of the nanofillers and compounding efficiency of the twin screw extruder.

1.2 Materials System

The material system that was utilized in developing the polymer nanocomposite comprises Nylon 645 and carbon nanofiber Pyrograph III (PR-24-XT-LH). The Nylon 645 served as the matrix and the Pyrograph III was used as the nanofiller for reinforcing the polymer matrix.

1.2.1 Polyamide 6 (Nylon 645)

Nylon 645 is an engineering thermoplastic monofilament that is ideal for fused deposition modelling 3D printing was chosen as the polymer matrix for the nanocomposites. Nylon 645 is a copolymer manufactured by Taulman 3D and consists of the purest form of a delta transition of Nylon 6/9, Nylon 6, and Nylon 6T. The choice of Nylon 645 as the polymer matrix for the nanocomposites stems from its good mechanical properties, high chemical resistance and is highly compatible in application where Nylon 6 and Nylon 6,6 are required.

1.2.2 Carbon nanofiber (PR-24-XT-LHT)

The nanoparticles used for polymerization in this study were pyrograph III, PR-24-XT-LHT grade. The LHT grade is a low heat treated (LHT) carbon nanofiber grade which has been carbonized chemically by heating to temperatures of 1500°C to deposit the carbon present on the surface of Pyrograf [18]. This heat treatment produces nanofibers which generally provides the highest electrical conductivity in nanocomposites. Pyrograph III-carbon nanofibers has a nanofiber density of 1.55 to 1.70 g/cc. Carbon nanofibers possess high length to diameter ratios which is essential for

achieving an electrical resistivity near the percolation threshold and can be viable to develop nanocomposites for static dissipation applications. In addition, its lower cost per pound as compared to other conductive nanofillers such as carbon nanotubes makes it more economically viable. Carbon nanofibers are also considered for the enhancement of the mechanical properties of the polymer matrix as carbon nanofibers also contain excellent intrinsic mechanical properties. Pyrograph III grade is an improved debulked carbon nanofiber for easy dispersion in the polymer matrix.

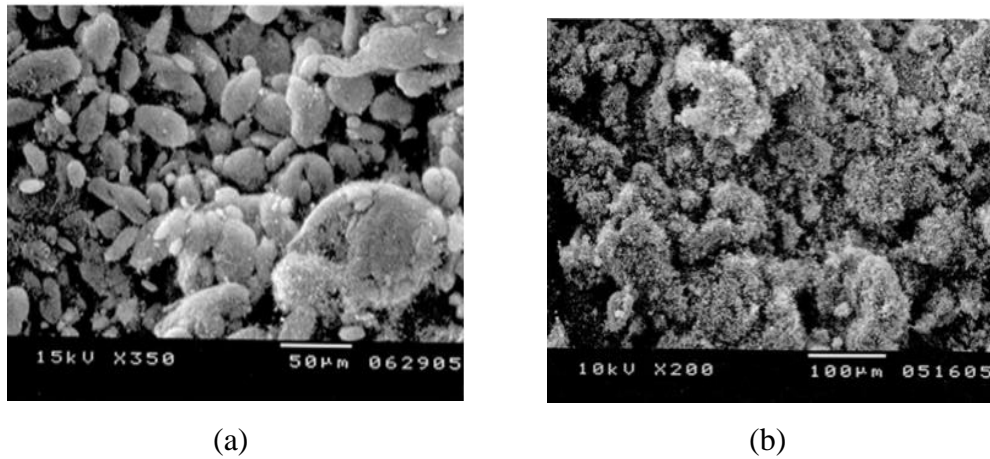


Figure 3: (a) Prior debulked CNF (b) “XT” improved debulked CNF [17]

1.3 Manufacturing

The manufacturing route was melt compounding via twin screw extruder to produce quality polyamide nanocomposite filaments for additive manufacturing. Additive manufacturing also, known as 3D printing. The 3D printing following subsection discusses the materials system and manufacturing techniques that will be employed in this study.

1.3.1 Melt compounding

The dispersion technique employed to produce the nanocomposite is a melt compounding process done using the aid of twin-screw extruder (TSE). TSE seems ideal for this process by exploiting the thermoplasticity of the host Nylon 645 matrix and could

effectively achieve an exfoliated dispersion state of the nanoparticles. Dispersion state of nanofillers in host polymers has been generally categorized into phase separated, intercalated and exfoliated and the exfoliated state has been identified as the most viable that could translate into best combination of desired materials properties [19].

TSE is a co-rotating intermeshing twin-screw extruder that consists of two parallel screws interlocked as much as possible rotating in the same direction and at the same circumferential speed. As shown in Figure 4, It comprises the intake zone to convey the solids, melting zone to soften the polymer, venting zone to remove volatiles and degassing purposes, mixing zone for distribution and dispersion and the metering zone for discharge control of the product

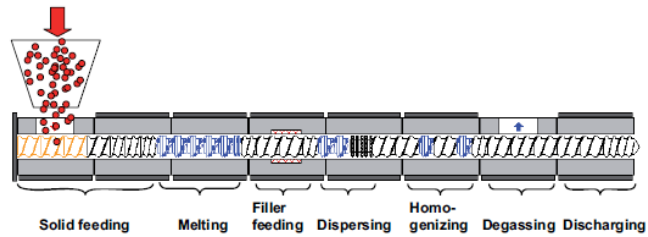


Figure 4: Melt Compounding Process [20]

1.3.2 3D Printing

The 3D Printing approach utilized in this research is an extrusion-based process commonly known as fused deposition modelling (FDM) which involves continuous layer-by-layer printing of thermoplastic filament to produce a 3D configuration. The working principle entails heating of the filament at the extruder nozzle to reach a semi-liquid state and then extruded on the platform or on top of previously printed layers as presented in Figure 5.

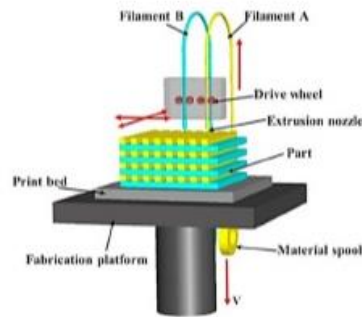


Figure 5: Fused Deposition Modelling 3D Printing

This 3D printing approach essentially depends on the thermoplasticity of the polymer filament which allows the filaments to fuse together during printing and then to solidify at room temperature after printing. The main process parameters that affect the structural integrity of the printed parts are layer thickness, layer width printing orientation. Defects such as air entrapment (in the same layer or between layers) and inter-layer distortion has been reported to be the primary cause of mechanical weakness [10]. The dominance of FDM approach in 3D printing stems from advantages such as low cost, high speed and simplicity, however limited number of thermoplastic materials and poor surface quality could pose a major drawback of this process.

2. EXPERIMENTATION

2.1 Materials Preparation

Nylon 645 was obtained as a monofilament for fused filament fabrication (FFF) 3D printing and it was pelletized using a mini industrial pelletizer. The compositional analysis of Nylon 645 is like that of Nylon 6 and it possess a high moisture sensitivity. Nylon 645 belongs to the Nylon family which are condensation polymers. They are synthesized by reacting an -H bond from a monomer with an OH bond to produce water, H₂O. During the synthesis, the water is dispelled in the manufacturing process, the two loose ends bond together and the resulting polymer is indeed water-resistant. However, due to the presence of amide group in their chain, Nylons are still moisture sensitive after a prolonged exposure to atmosphere and could lead to hydrolysis of the condensation polymer [21]. All nylons will re-absorb humidity from the surrounding air within just 18 hr. and the rate of moisture absorption at 50% relative humidity at room temperature is 2.8.

The Nylon 645 pellets were needed to be pre-dried prior to the extrusion process to remove any accumulated moisture. The presence of moisture is detrimental to the intrinsic properties of the polymer since the presence of excess water molecules would disrupt the water bond in the polymer chain and could lead to chain breakage. The pellets were dried using a Vacuum Dryer as shown in Figure 6. The vacuum drier is most suitable as it offers a more time efficient drying of the pellets and avoids excessive drying for heat sensitive materials like Nylons. The drying parameters are important because excessive drying would increase the viscosity of the extrudate and could lead to frictional heat generation during the extrusion process. In order to maintain an efficient extrusion

process, the pellets were dried at a temperature of 180°F and the drying time was scheduled between 6 to 10 hours.



(a) (b)
Figure 6: (a) Nylon 645 Pellets (b) Vacuum Dryer

2.2. Twin Screw Compounding

The polymer nanocomposite was compounded via twin screw extruder. This was achieved with the help of Process 11 twin-screw extruder manufactured by Thermo Fisher Scientific. The compact co-rotating 11mm twin screw extruder, as presented in Figure 7a, is designed with a unique monocoque housing that is suitable for compounding thermoplastic polymers. The extruder is connected to an appropriate chiller unit for reducing internal heat losses and barrel cooling function. It comprises 2 separate volumetric hoppers for feeding the constituent's materials. In addition to its water-cooled primary feed port it contains 3 multifunction barrel ports for additional feeding and venting purposes. Its barrel is separated into 8 sections to facilitate temperature profiles. The barrel diameter is 11mm, barrel length of 440mm and a L/D ratio of this extruder is 40.

The standard helix elements of the twin screws are broadly categorized into the conveying, mixing and extrusion elements as presented in Figure 7b. The conveying elements are self-wiping in nature and are used in the feeding and venting section of the

screw arrangements. The mixing section in the configuration are made up of combination of several multiple mixing elements in 0 or 90° orientation. In addition, the 0 and 90° mixing elements can be alternated to form 30° and 60° orientation in the mixing section. The mixing and conveying properties can be varied by monitoring the offset values between the neighboring mixing elements. The mixing properties increases with increasing offset values – an extreme 90° offset section and the conveying properties can be increased at a lower offset value of 30° and 60°. The extrusion elements consist have a single lead geometry to generate the extrusion pressure. The mixing, conveying, and extrusion elements has a pitch of 1 L/D, 1/2 L/D and 1 1/2 L/D, respectively.

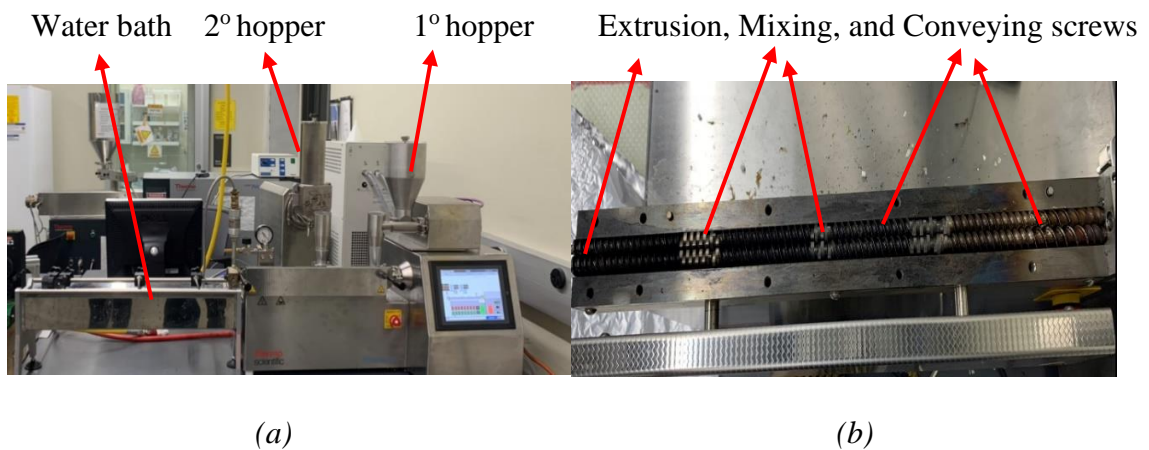
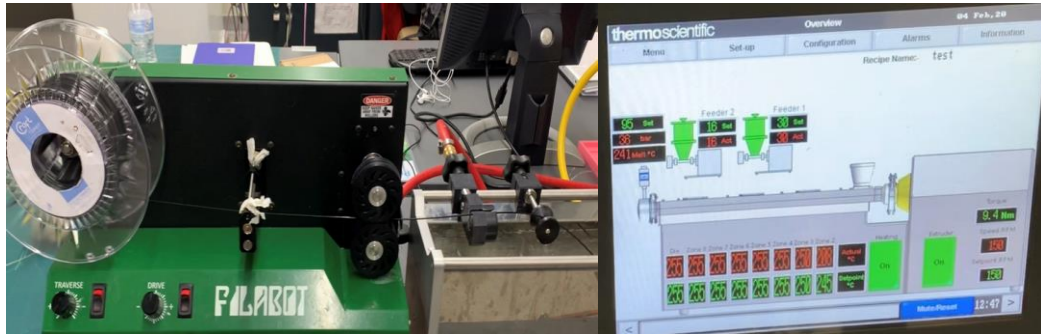


Figure 7: (a) Twin Screw Extruder (11mm diameter) (b) Twin Screws Elements

2.2.1 Dispersion of carbon nanofiber

The primary feeder was used to feed the nylon 645 pellets and the CNF nanoparticles was fed downstream along the barrel via the secondary hopper. The dried nylon pellets were first fed in the primary hopper and then carbon nanofibers was side fed at a distance of 18D from the primary hopper to ensure proper mixing with the molten nylon. The extruder barrel comprises of 8 sections to facilitate temperature profiles along the extruder barrel and the melt temperature was maintained between 245-255 °C as

shown in Figure 8b. The screw rotational speed was maintained at 150 rpm to facilitate adequate shear loading and the optimized extrusion parameters used to obtain a consistent filament of 1.75mm diameter at various loading levels of CNF are presented in Figure 9. The compounded nanocomposites filaments were cooled downstream in a water-bath attachment and a Filabot Spooler (shown in Figure 8a) was used for winding the extruded filaments for the FDM process.



(a) (b)
 Figure 8: (a) Filabot Spooler (b) Control Screen

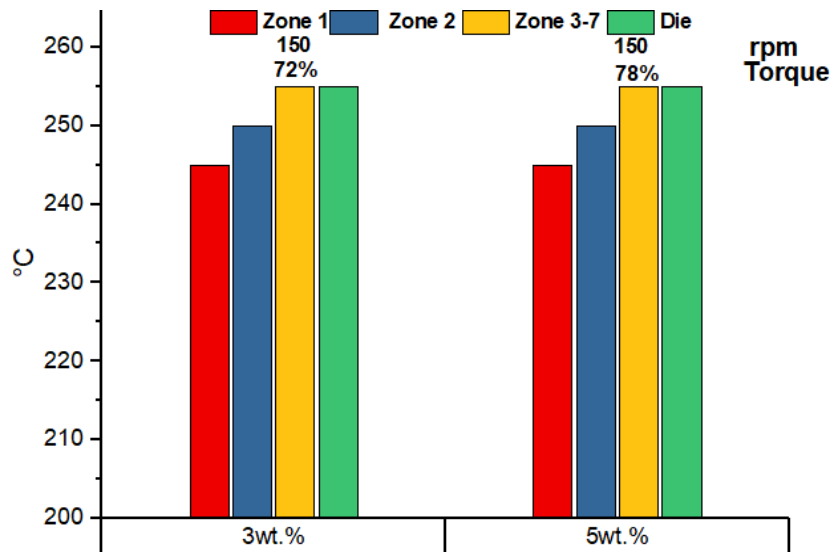


Figure 9: Twin-screw Extrusion Parameters

The feed rate of the primary hopper containing the nylon pellets was maintained at 30 rpm and using this feed rate, 3 and 5 wt.% loading of the carbon fiber was achieved at 12rpm and 16rpm respectively according to mathematical relationship in Equation 1.

$$Z = \frac{X \text{ (Solute)}}{X+Y \text{ (Solution)}} \quad (1)$$

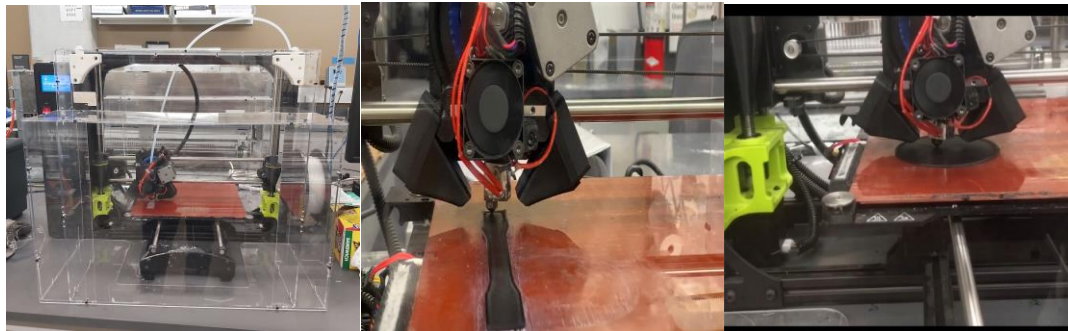
Z = amount of carbon nanofiber in weight percent (3 and 5 wt.%)

X= amount in grams at 30rpm in 1 minute for nylon pellets

Y= amount in grams at 12 and 16 rpm in 1 minutes for 3 and 5 wt.% respectively.

2.3 Fused Deposition Modelling

The PA6/CNF nanocomposites were FDM 3D printed using commercial-off-the-shelf (COTS) 3D printer, Lulzbot TAZ 6 as presented in Figure 10. The LulzBot TAZ 6 was used to print tension, flexural, DMA, and resistivity test samples of the nanocomposite filaments at a loading level of 0%, 3%, and 5%. It is noteworthy that the 3D printing was done under same printing conditions for all printed nanocomposites with varying CNF loading for direct comparison. Also, the FDM printing parameters were optimized for better printability.



(a)

(b)

(c)

Figure 10: 3D printing (a) Enclosure Box (b) of Tensile Samples (c) of ESD Samples

2.3.1 Printing parameters

The optimized printing parameters for the FDM process is presented in Table 3. The printing temperature was maintained at 260 °C to ensure proper deposit viscosity and flowability of the filament. Nylon 6 could in order to facilitate good bed adhesion of Nylon, a bed temperature of 100°C was selected to ensure a successful foundation print. The outer edge speed was selected to be about half of the infill speed and the line width, and an infill overlap was selected to ensure proper interlayer bonding. Extruder nozzle size of 0.8mm was selected to avoid clogging due to the high aspect ratio of the carbon nanofibers. The test samples were printed at 0, 90° orientation in the XY plane to maximize the part strength

Table 3: 3D Printing Parameters of PA6/CNF Nanocomposites

Printing Conditions	Numeric values
Nozzle Temperature	260
Bed Temperature	100
Nozzle Diameter	0.8mm
Layer height	0.2mm
Layer width	0.75
Print Infill	100%
Infill overlap	0.2mm
Print Speed	Infill= 50 mm/s, Wall= 25mm/s
Printing pattern	0, 90°
Flow rate	100%

3. MATERIALS CHARACTERIZATION

3.1 Microstructural Investigation

The performance of a developed nanocomposite is identified to be dependent on the exfoliation of the nanofillers in the host polymer during dispersion. The nanoparticles in their natural state does not adhere to the polymer matrix, instead bond to themselves, thereby clustering together to form agglomerates. This is an undesirable event that could results into a deterioration of materials properties. Therefore, it is imperative to obtain a representative view of dispersion state of the nanofillers in the polymer matrix. This was achieved by subjecting the material to a microstructural investigation using the field emission scanning electron microscope presented in Figure 11. This was carried out by scanning certain cross section of the test sample with a focused electron beam. The focus electrons excite the surface of the sample, thereby resulting into signal information regarding the composition and surface morphology of the sample. The signal information and the position of the beam provides the SEM image[22].



Figure 11: Field Emission Scanning Electron Microscope (FE SEM)

3.2 Mechanical Testing

The mechanical testing that was carried out are tensile and flexural testing to measure the mechanical stiffness and strength of the nanocomposites. The mechanical strengths indicators are closely related as they both measure the resistance of the nanocomposite to deformation; however, the applied load differs.

3.2.1 Tensile testing

Total five tension samples were printed according to ASTM D638-Standard Test Method for Tensile Properties of Plastics [23]. The tensile dog bone specimen “Type 1” has overall length, overall width, and thickness as 165mm, 19mm, and 3.2mm, respectively. The tensile testing was performed as shown in Figure 12 using United Testing Machine (UTM) with a 50kN loading capacity (11 kips) and the strain values were collected using 2 inches gauge length extensometer with a measuring accuracy of 0.0002. The force-extension data was generated using the Datum 5i software of the UTM and tensile properties were evaluated.



Figure 12: Tension test of 3D Printed PA6/CNF Nanocomposites

3.2.2 Flexure testing

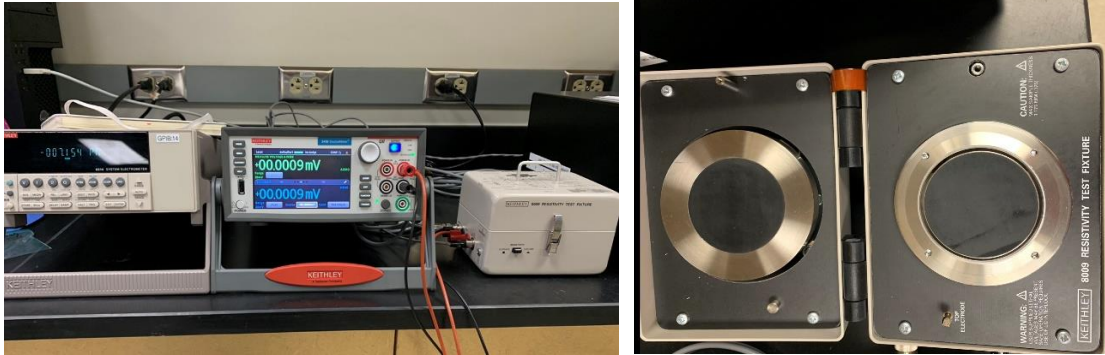
Total five flexural samples were printed and subjected to a 3-point bed test according to “ASTM D790- Standard Test Methods for Flexural Properties of Unreinforced and Reinforced Plastics and Electrical Insulating Materials” [24]. The flexural samples with a dimension of 12.7 mm wide, 3.2 mm thick, and 127 mm long were tested on the support span (span-to-depth ratio) of 16:1. These tests were performed according to Type I, which utilized the cross head position as the deflection measurements and Procedure B was followed, which is designed principally for those materials that do not break or yield in the outer surface of the test specimen within the 5.0 % strain limit when Procedure A conditions are used.

3.3 Electrical Testing

The electrical resistivity of control and nanomodified samples was measured according to ASTM D257 – “Standard Test Methods for DC Resistance or Conductance of Insulating Materials [25]. This is to evaluate the volume resistivity of the CNF conductive fillers. The test samples printed were circular disks with a dimension of 1mm thickness and 88.9 mm diameter. The volume resistivity was measured by Keithely Megohmmeter setup (as presented in Figure 13) comprising the Keithely 2450 source meter, Keithely 6514 Electrometer and the Linear 2-point probe (Jandel Universal Probe) for housing the test sample. Voltage varying from 10V to 120 V was applied using the source meter for an electrification time of 60 seconds and the amount of current flowing was sensed by the electrometer. The volume resistivity values were evaluated according to the mathematical relationship presented in Equation 2.

$$\rho_v = k_v * \frac{R}{t} \quad (2)$$

Where ρ_v = volume resistivity ($\Omega \cdot \text{cm}$),
 k_v , effective area of the circular electrode = 22.881 cm^2 ,
 R = measured resistance (Ω), and t = sample thickness (1mm).



(a) (b)
Figure 13: (a) Keithley Megohmmeter Setup (b) Effective Circular Electrode

3.4 Thermal Analysis

The material thermal stability was evaluated via ASTM - Standard Test Method for Thermal Stability by Thermogravimetry [26]. This was to determine the decomposition temperature of the materials and the degree of mass change via thermogravimetry. The mass of the sample was about 7.5mg for nanomodified composites. The samples were placed inside an alumina pan at ambient temperature after zeroing an empty and clean specimen pan. The test material was heated from ambient temperature to 600 °C at a rate of 10 °C/min. The testing material was heated in an alumina pan and maintained under inert atmosphere of 99.9% purity, purging the inert gas (Nitrogen) at a rate of 50 ml/min.

Thermal transitions of the nanomodified polyamide 6 were investigated via ASTM D3418-15-Standard Test Method for Transition Temperatures and Enthalpies of Fusion and Crystallization of Polymers by Differential Scanning Calorimetry (DSC)[27]. This test method was employed to evaluate the glass transition temperature, peak crystallization temperature and melting point of the material. The testing procedure was a

single testing as discussed in the thermogravimetry procedure and was carried out with the aid of simultaneous differential thermogravimetry (SDT) analyzer (shown in Figure 14a) capable of both TGA and DSC. The DSC sensing device of the SDT was used to monitor the difference in heat input between a reference material and a test material due to energy changes in the material, thereby resulting into different exothermic valleys and endothermic peaks, indicating different thermal transitions.

Dynamic mechanical data of the carbon nanofiber modified polyamide 6 was investigated according to ASTM D4065- Standard Practice for Plastics: Dynamic Mechanical Properties: Determination and Report of Procedures [28]. This test was aimed to determine the viscoelastic characteristics of the material by monitoring the elastic and loss modulus as a function of temperature. A rectangular cube with dimension 35mm X 12mm X 3 mm, maintained at a temperature of 23° C was subjected to a mechanical oscillation of a frequency of 1 HZ in a single cantilever test mode. The material was taken through a temperature ramp from 23° C to 200° C at a rate of 5 ° C/min via a Dynamic Mechanical Analyzer equipment TA- DMA 2980 (shown in Figure 14b) and the obtained data was analyzed using Universal Analysis Software.



(a)

(b)

Figure 14: (a) Simultaneous Differential Thermogravimetry-SDT 650

(b) Dynamic Mechanical Analyzer- DMA 2980

4. RESULTS AND DISCUSSION

4.1 Microstructural Evaluation

The scanning electron micrographs obtained from microstructural investigation are presented in Figure 15. Having known that the host Nylon polymer is intrinsically insulative, the nanocomposite was sputter coated by bombarding the target sample with 20nm of carbon thin film to increase the samples electrical conductivity. The conductive carbon thin film enhances the emission of the SEM secondary electrons and reduces thermal damage by avoiding the charging of the sample. As shown in Figure 15, it is suspected that the micrograph at 3 wt.% shows slight distinct features of the carbon nanofibers but nothing could be observed in that of 5 wt.%. At this point, it is hard to tell the distinctive features and dispersion state in the nanocomposites and a higher magnification microstructural investigation like transition electroscop microscope (SEM) is highly recommended.

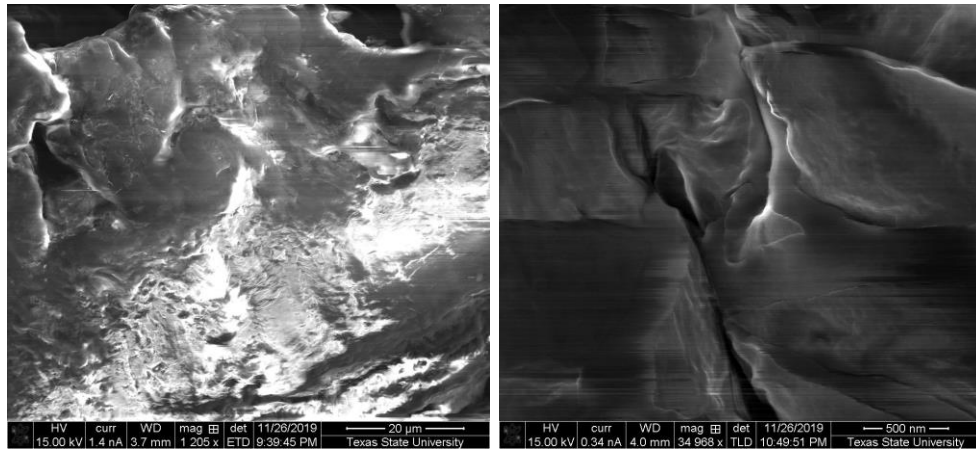


Figure 15: SEM images of (a) 3wt% (b) 5wt% 3D Printed PA6 Nanocomposites

4.2 Mechanical Properties

The mechanical response of the investigated material is of prime importance in quantitatively evaluating the structural integrity of the 3D printing nanocomposite filaments. This could prove viable as a fabricating 3D printing filament for end use industrial products, thereby replacing injection molded parts. The mechanical properties evaluated are the tensile and flexure properties as presented in Table 4.

Table 4: Mechanical Properties Data

	0 wt.% CNF	3 wt.% CNF	5 wt.% CNF
Ultimate Tensile Strength	37.21	41.44	30.14
(MPa)	(2.108)	(1.836)	(6.512)
Tensile Modulus	1.574	2.943	1.559
(GPa)	(0.074)	(0.905)	(0.171)
Percentage of Elongation	78.90	46.30	34.45
(%)	(0.055)	(0.107)	(0.229)
Equilibrium Toughness	1.4649	2.051225	1.20574
(MJ/m ³)	(0.158)	(0.649)	(0.083)
Flexural Strength	33.93	39.54	40.39
(MPa)	(5.331)	(3.340)	(6.53)
Flexural Modulus	0.768	1.130	1.173
(GPa)	(0.133)	(0.115)	(0.243)

***Standard Deviation in Parenthesis**

Figure 16 illustrates the trend in tensile and flexural strength of the investigated material. The trend in the observed tensile and flexural strength are presented graphically in Figure below to show the trend in relation to the reported data given in Table 4. The tensile strength was observed to have appreciably increase at 3wt% CNF inclusion, which decreases as the CNF concentration was increased to 5wt%. It is well understood that high aspect ratio fillers like CNF and CNT prove difficult to disperse homogeneously because of their high surface area and a strong inclination to agglomerate [29]. Due to this reason, high shear dispersion techniques like twin screw extrusion has been recommended. However, the high shearing action associated with this technique could truncate the long fibers, thereby reducing its aspect ratio below a critical value. This could explain the deterioration of tensile strength observed at 5wt%. Although the tensile strength depreciates at 5wt%, the continuous improvement in the flexural strength of the nanocomposites is an indication that inclusion of CNF could prove viable in enhancing mechanical properties of nanocomposites. These mechanical strengths indicators are closely related as they both measures the resistance to deformation depending on the type of applied load.

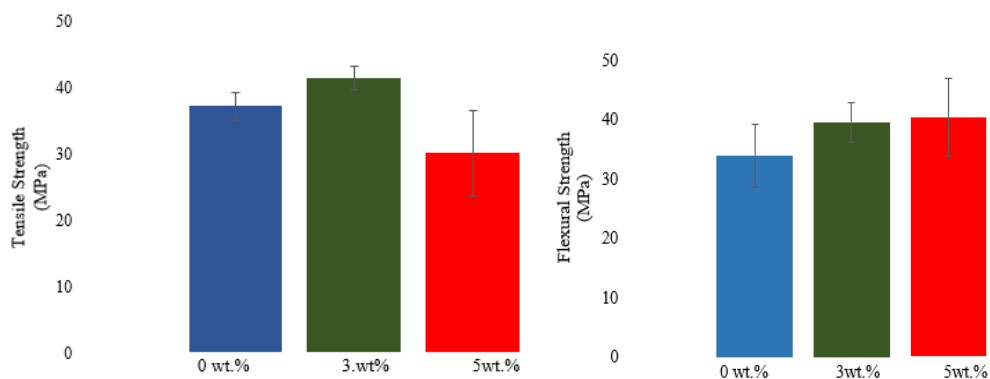


Figure 16: Tensile and Flexural Strength of 3D Printed PA6/CNF Nanocomposites

Barrick (2011) reported that improvement in tensile properties of nanocomposites is dependent on the length to diameter ratio (aspect ratio) and the nanofiber-matrix interfacial strength. According to Figure 17, addition of 3wt.% CNF exhibits a strong reinforcing and stiffening effect of the Nylon matrix and the enhancement observed in tensile modulus could be attributed to a strong interfacial strength which effects an efficient load transfer from the matrix to the reinforcement [30]. By increasing to 5wt% CNF inclusion, no appreciable effect was observed, however the nylon matrix was increasingly stiffened by increasing CNF contents under bending load. The spatial orientation of carbon nanofibers significantly impedes the movement of the amorphous phase of the Nylon matrix, thereby resulting into the stiffening of the material. It is noteworthy that higher loading levels is prone to entanglements of the fibers, promote agglomeration and consequently deteriorating the stiffness of the nanocomposites. Therefore, it is imperative to optimize the processing parameters of the extrusion process to maximize the reinforcing ability of CNF at high loading levels, like 5wt.% and above

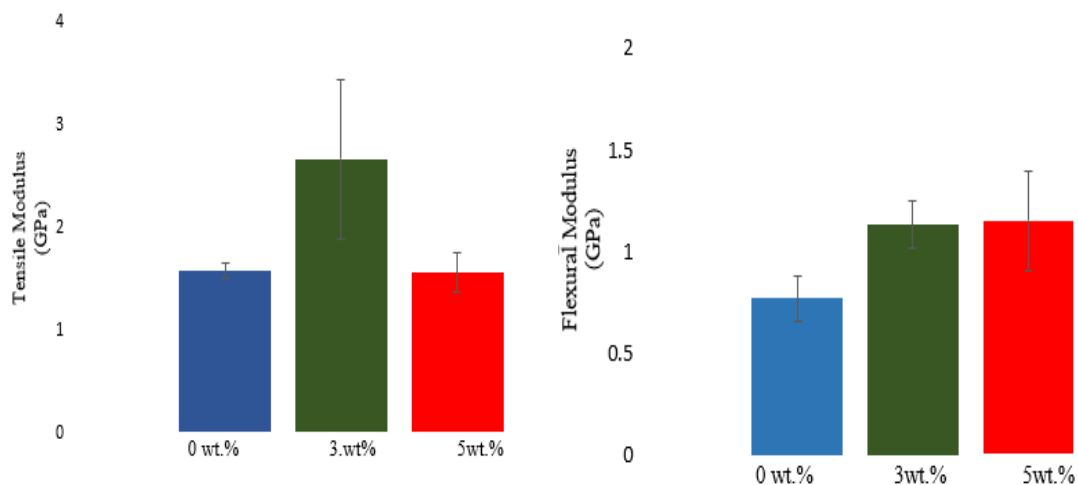


Figure 17: Tensile and Flexural Modulus of 3D Printed PA6/CNF Nanocomposites

Figure 18 illustrates the percentage elongation and the toughness values of the nanocomposite filaments. The percentage elongation reduces drastically with increasing CNF loading. % elongation is an indication of the ductility of the material and the continuous decline could be attributed to the restriction in the polymer chain movement. This restriction has been suggested to be due to the reduction in the free volume capacity of the Nylon 6 [30].

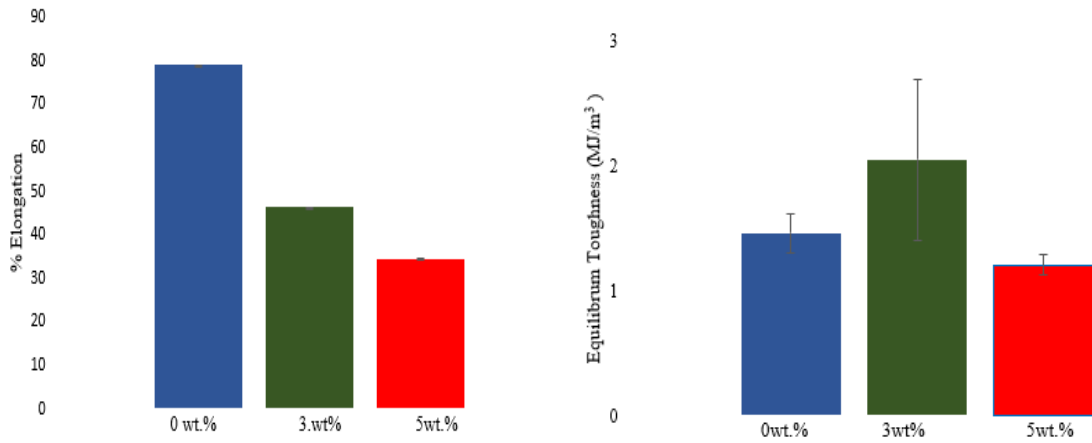


Figure 18: % Elongation and Toughness of 3D Printed PA6/CNF Nanocomposites

Figure 19 shows the tensile stress versus tensile strain plots which was obtained by integrating from zero to elongation at break to illustrates the area under the tensile curve. The area under the stress-strain curve was evaluated as the equilibrium toughness which represents the total strain energy per unit volume that was induced by the applied stress. The similarity in the trend showed in the equilibrium toughness and tensile strength is an indication of the close relationship between the two tensile properties, which explains the fact that maximizing the strength is parallel to improving the toughness of the nanocomposites.

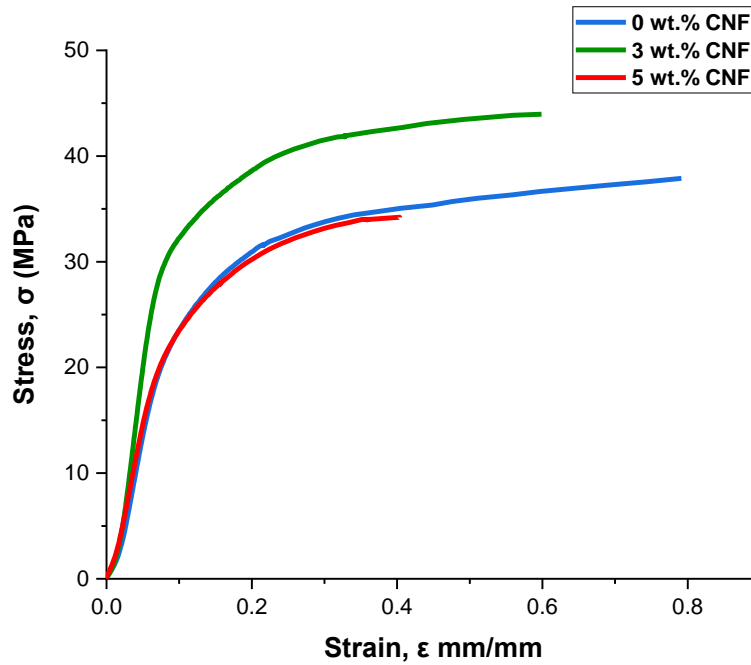


Figure 19: Tensile stress vs Axial strain of 3D Printed PA6/CNF Nanocomposites

4.3 Volume Resistivity

Table 5 presents the volume resistivity data collected in an electrical resistivity testing by varying the voltage source from 10-120 v. The primary importance for measuring the volume resistivity is to evaluate how the carbon nanofiber impart the conductivity of the Nylon matrix which could prove viable in low resistivity applications such as static dissipation. The conductivity of the nylon matrix is achieved via the attainment of a percolation nexus of CNF, which creates a conductive pathway throughout the matrix, thereby facilitating electron transfer [31]

Table 5: Volume Resistivity Values

Resistivity (Ohm.cm)			
Voltage (V)	3wt%	5wt%	0wt%
10	6.21E+11	1.75E+12	5.40E+13
20	6.27E+11	1.52E+12	5.40E+13
30	7.79E+11	1.43E+12	5.40E+13
40	7.04E+11	1.38E+12	5.40E+13
50	7.33E+11	1.36E+12	4.35E+13
60	7.30E+11	1.33E+12	4.46E+13
70	5.46E+11	1.32E+12	4.48E+13
80	5.16E+11	1.30E+12	4.55E+13
90	5.08E+11	1.29E+12	4.40E+13
100	5.23E+11	1.31E+12	4.45E+13
120	5.06E+11	1.30E+12	4.30E+13

The trend in the volume resistivity values with increasing CNF inclusion is presented in Figure 20. It could be observed that the volume resistivity of the Nylon 6 matrix in the order of 10^{13} was lowered to the order of 10^{11} and 10^{12} for 3 and 5 wt.% respectively. In CNF nanocomposites, the tunneling effect facilitated by the high aspect ratio of the filler has been identified as the main mechanism of electrical conduction[32]. The observable reduction in the resistivity could be as a result of a conductive network being formed by the CNF, where electrons can tunnel along the length of one filler to another, thereby overcoming the high resistance imposed by the nylon matrix. In order to maximize the conductive ability of CNF, it is imperative to maintain its high aspect ratio.

This could give an insight into the slight decrease of resistivity value observed at 3 wt. and 5wt.%. It is suspected that the CNF could have suffered from high shear forces of the twin-screw compounding process, resulting into shortening of the long fibers and consequently delaying the onset of electrical percolation. Although, the results obtained does not reflect a significant influence of the conductive CNF, the resistivity of 3wt.% still falls within the allowable resistivity values for ESD compliance rated between 10^{10} - 10^{12} ohms.cm [33].

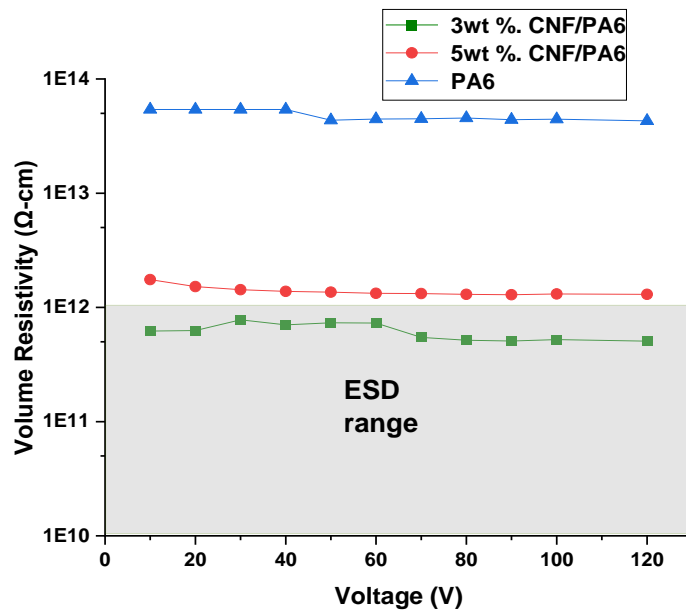


Figure 20: Volume Resistivity of 3D Printed PA6/CNF Nanocomposites

4.4 Thermogravimetry

The thermogravimetry aspect of the SDT illustrates the thermal stability by measuring the weight loss as a function of temperature. TGA is of prime importance in evaluating the thermal stability of the nanocomposites and the TGA analysis results are presented in Table 6. There is a close relationship between the thermal stability and the structural integrity of materials which require understanding the decomposition kinetics of our material in a temperature-controlled environment.

Table 6: Thermogravimetric Analysis

Thermal properties	0 wt.% CNF	3 wt.% CNF	5 wt.% CNF
Decomposition Temperature (°C)	400.95	402.53	402.68
Weight % loss	97.738%	97.357%	96.832%

The TGA curve in Figure 21 illustrates the onset decomposition temperature and the weight percent loss of the nanocomposites at the end of the heating profile. The extrapolated onset temperature signifies the temperature at which the weight loss begins which is an indication of the thermal stability of the material. The observed slight increase in thermal stability with increasing CNF content could be attributed to the restriction of the Nylon macromolecules by the network structure of the CNF. The intrinsic high thermal conductivity of CNF prevents any sort of heat accumulation and conducts heat uniformly, thereby increasing the thermal stability of the Nylon matrix. In addition, strong interfacial adhesion has been identified as a reason for the thermal stability of CNF based nanocomposites[29]. Strong interfacial bonds prevent the occurrence of interstices that could occur under thermal stresses where the diffusion of volatile gases from the decomposing material is prominent. However, the interface is prone to interstices buildup at higher CNF loading. Furthermore, no major degradation was observed with inclusion of CNF on the TGA curve and the thermal stability of the nanocomposites was sustained throughout the scanning temperature. The weight loss percentages at the final temperature reduces with increasing CNF loading and the pristine nylon being the highest with 97.758%. The reduction in weight loss could be ascribed to the restriction imposed by the CNF network structure, preventing the mobilization of the gaseous nylon macromolecules to encounter outer atmosphere during degradation [34].

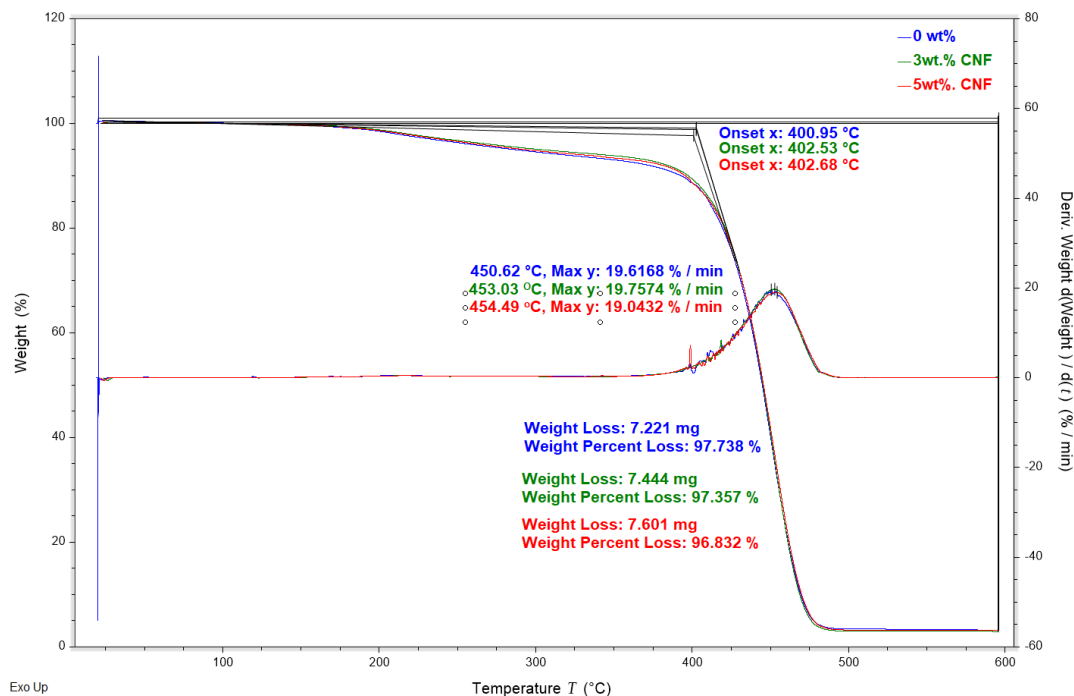


Figure 21: TGA/DTGA Curve of PA6/CNF Nanocomposites

In order to clearly understand any form of overlapping reaction and the peak temperature at maximum weight loss measurement, the first derivative of the TGA curve was done to obtain the differential thermogravimetric analysis (DTGA) of the nanocomposites. The DTGA curves as presented in Figure 21 was generated as the first derivative of the weight with respect to temperature or time. The peak of the first derivative curves, also known as inflection point, signifies the point of maximum rate of change on the weight loss curve. It could be observed from the DTGA curves that there was a delay of the derivative peak temperature in the 3 and 5 wt.% CNF modified nanocomposites. This trend is also in consistent with the initial observed trend of the onset decomposition temperatures which presumes a higher thermal stability of the nanocomposites as compared to the host PA 6.

4.5 Differential Scanning Calorimetry

Table 7 highlights the thermal transition obtained in the DSC first heat cycle of the investigated material. DSC is an important technique that can be used to qualitatively and quantitatively characterize the thermal transitions unique to a material. These thermal transitions are important in monitoring the materials thermal behaviour in different service temperature.

Table 7: DSC Thermal Transitions

Transition parameters	0 wt.% CNF	3 wt.% CNF	5 wt.% CNF
Glass Transition (°C)	59.39	60.35	59.93
Peak crystallization (°C)	171.61	167.42	166.81
Melting temperature (°C)	214.35	213.31	213.32
Heat of crystallization (J/g)	52.53	77.34	77.43
Degree of Crystallinity (%)	22.8	34.6	35.4

Figure 22 presents the DSC scan of the nanocomposites. The first observable signal on the DSC scan is the glassy region which signifies the temperature region where the amorphous portion of the material is moving from a glassy to a rubbery state. The glass transition temperature (T_g) of the neat matrix occurs at 59.93°C and a minimal increase to 60.35 and 59.93 °C was observed at 3 and 5 wt.% reinforcement respectively. Dispersion of CNF within the Nylon matrix led to reduction in free volume movement of the polymer macromolecules due to the restriction imposed by the CNF, thereby delaying the onset of glass transition. The slight increase in T_g of the amorphous region of the

Nylon/CNF composites is an indication of the polymer molecules interlocked into a rigid amorphous structure which could possibly translate to the enhancement of the mechanical properties of semicrystalline nylon matrix. In a semicrystalline polymer like Nylon, the amorphous region is reported to be responsible for the elasticity phenomenon [35]. During applied tensile stress, the amorphous molecular chain deforms elastically and the crystalline domains remains undisturbed until yielding begins. The presence of this amorphous region delays the onset of the plastic deformation of the crystalline phase, thereby resulting in the improvement of the strength and modulus of the semicrystalline polymer. Furthermore, the T_g could be used to predict the service temperature of polymeric materials depending on application and desired physical properties, especially for fully amorphous polymers. However, it is noteworthy that the Nylon 6, a semicrystalline polymer, being investigated in this study does not soften even above the T_g . This could be attributed to the presence of relatively strong intermolecular forces which is more sensitive to higher temperature, like melting temperature[36]

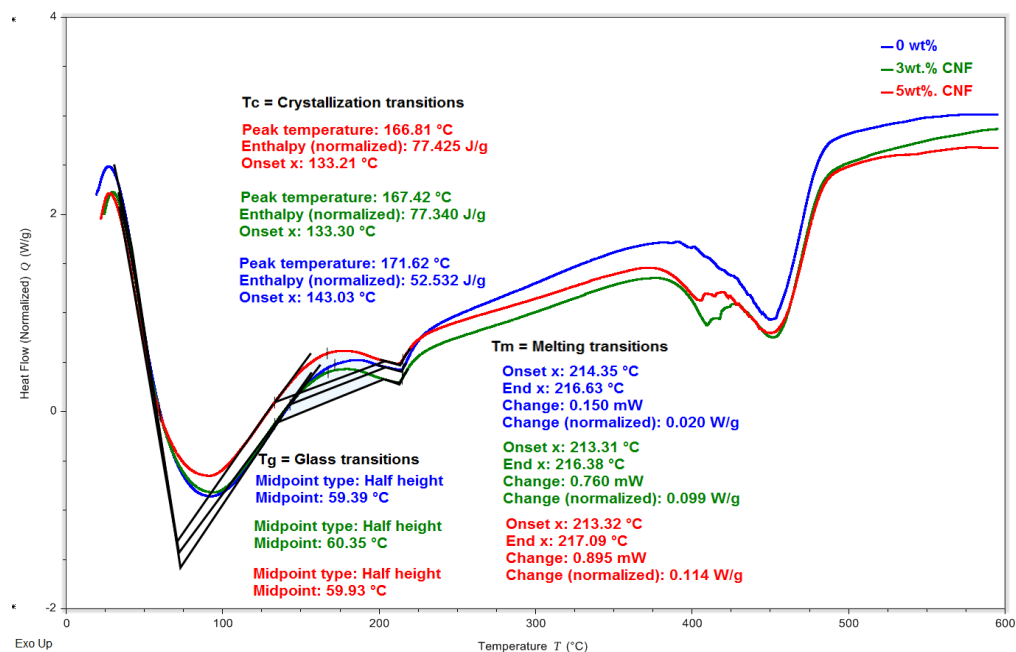


Figure 22: DSC Scan of PA6/CNF Nanocomposites

The transition peak after the T_g illustrates the crystallization behavior of the investigated material system. The peak crystallization temperature was observed to be highest for the neat Nylon matrix, however, there was an early onset of crystallization at 3 and 5 wt.% respectively. This is expected and it is consistent with the Hoffman's nucleation theory which describes polymer crystallization in terms of kinetics and thermodynamics of surface nucleation[37]. The addition of CNF creates new surfaces in the nylon matrix thereby reducing the total surface energy of nuclei formation and consequently promoting heterogeneous nucleation which possesses a lower Gibbs free energy for crystallization. The heat of crystallization is the enthalpy associated with the crystallization process and could be used to determine the degree of crystallinity in the investigated material according to the following equation [34].

$$X_c (\%) = (\Delta H_m / (1-\phi) \Delta H_o) \times 100 \quad (3)$$

Where ΔH_m is the enthalpy of crystallization melting shown in the figure above, $\Delta H_o = 230 \text{ J/g}$ is the consensual value reported in literature for the enthalpy of fusion of 100 % crystalline PA6 [38]. Using equation (1) the $X_c (\%)$ values have been computed as 22.8%, 34.6% and 35.4% of 0, 3 and 5 wt.% respectively of CNF loading. The observed increasing trend affirms the heterogeneous nucleation promoted by the carbon nanofibers. It is suspected that the higher degree of crystallinity experienced at 3 and 5wt% loading levels translated into the improvement of thermal stability and mechanical properties. However, the unusual deterioration of tensile properties of 5wt% could be due to possible weak interfacial strength vis-à-vis agglomeration effects.

The melting transitions illustrates the onset of melting of the investigated material system. It could be observed that the onset of melting temperature slightly decreases with

increasing CNF loadings. The presence of second phase CNF could promote increase in dislocation movements in the Nylon Matrix in form of interstices. These interstices could be perceived as weak impurities which could lower the melting temperature of the Nylon/CNF composites.

4.6 Dynamic Mechanical Analysis

The DMA was used to evaluate the ability of the investigated material to return or store energy (storage modulus G'), dissipate energy (loss modulus G'') and the ratio of these effects ($\tan \delta$) signifies the transition from the glassy to rubbery state of the material. The dynamic thermomechanical response observed in Figure 23 is quite like the tensile modulus observation. At 3wt.% loading of CNF, an improvement in the G' throughout the scanned temperature is an indication of the stiffening ability of CNF on the nylon matrix. The enhancements of storage modulus at 3wt% and 5wt% was more prominent at higher temperature, indicating the ability of CNF to enable the Nylon matrix to sustain its stiffness. This has been suggested to be due to interfacial interlocking between CNF and the polymer matrix which contributes to an additional reinforcement of restricted matrix molecular chain movement in the interface region of the nanocomposite[39]. The rapid decline in storage modulus in the transition region observed with increase in temperature could be attributed to a collective segmental motion of the chains in the polymer backbone, resulting into an energy dissipation phenomenon.

Figure 24 presents the loss modulus of the nanocomposites at the end of the heating cycle. The loss modulus is an out-of-phase response which measures energy absorbed due to relaxation. The peak position of the loss modulus did not shift

significantly at 3wt%, signifying that the inclusion of CNF has an insignificant effect on the dynamic relaxation behavior of the Nylon matrix [40]

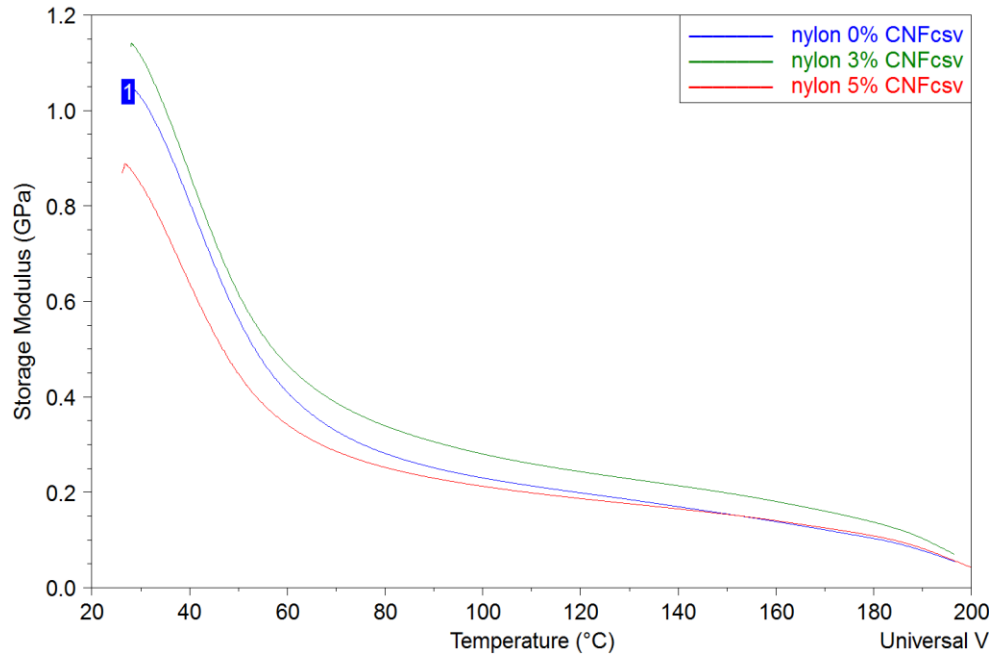


Figure 23: DMA Thermograms of Storage Modulus – Temperature Profile

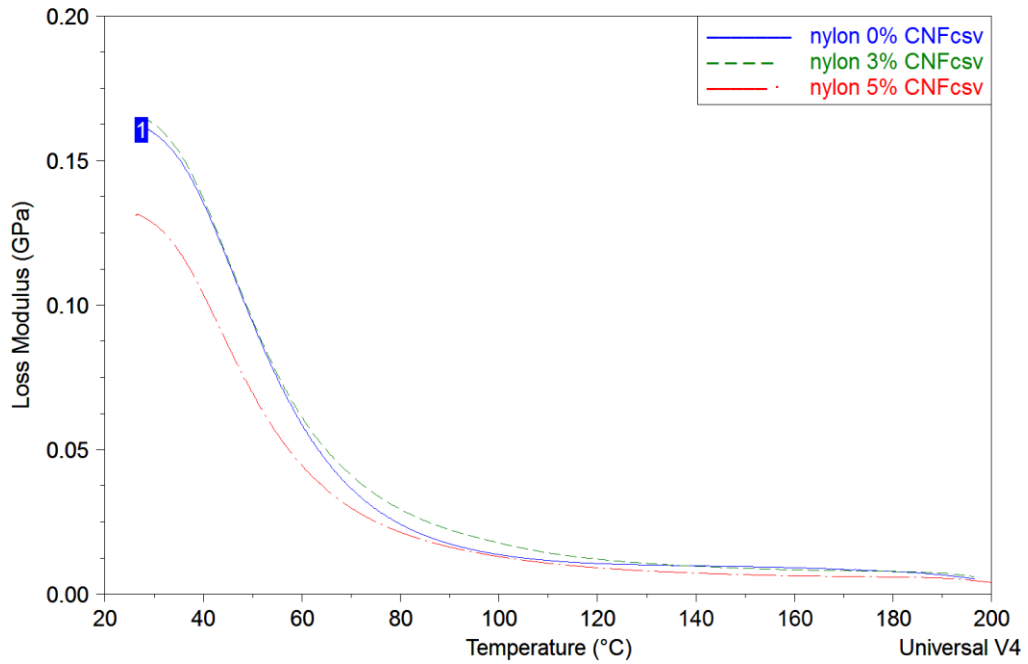


Figure 24: DMA Thermograms of Loss Modulus – Temperature Profile

The damping behavior of the investigated material were evaluated by the tangent of the phase angle (Tan Delta). Damping behavior measures the ability of a material to absorbs energy. This is an important attributes of condensation polymers like polyamides which could be attributed to their high impact strength. According to Figure 25, it could be observed that the peak of the tan delta curves did not shift significantly with addition of carbon nanofibers. This behavior is an indication that the damping behavior of the PA 6 was sustained during the heating temperature profile. Also, it could be observed that the area under the tan delta curve reduces with increasing CNF contents. This behavior could be attributed to a homogeneous thermal energy distribution within the nylon/CNF nanocomposites that results from the high differential thermal conductivity between the CNF and Nylon matrix [34].

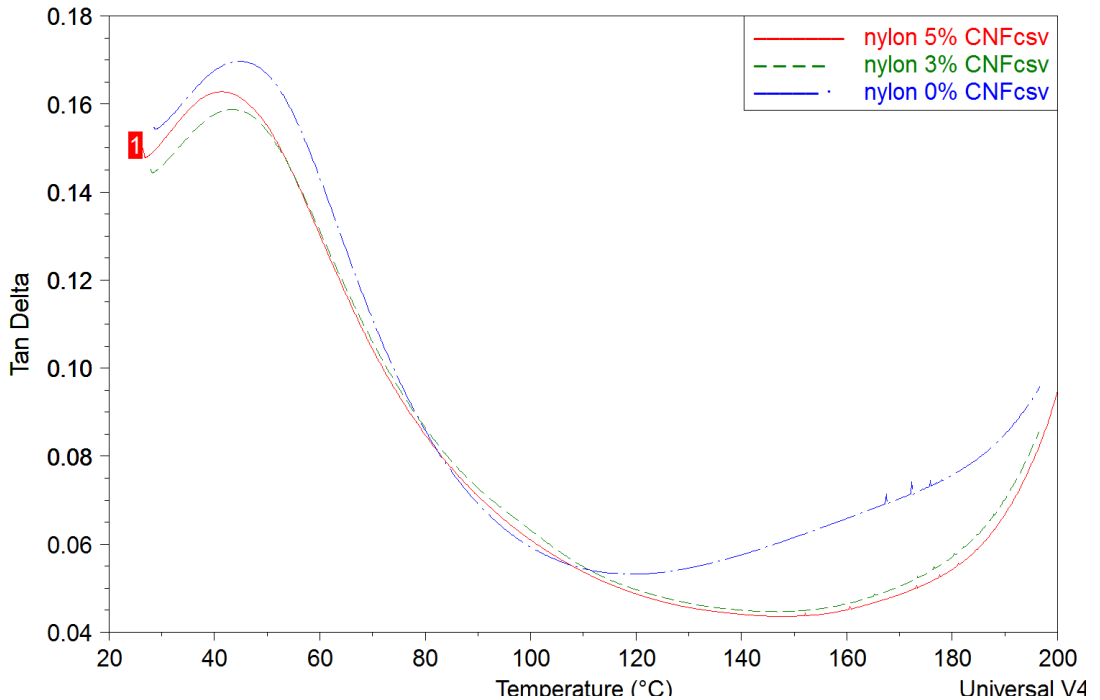


Figure 25: DMA Thermograms of Tan Delta – Temperature Profile

5. CONCLUSION AND RECOMMENDATION

5.1 Conclusion

PA6/CNF nanocomposite was successfully developed for 3D printing using co-rotating twin screw extruder for the compounding process. The twin screw compounding process was used to produce a 1.75mm diameter of nanocomposites filaments for the 3D Printing FDM process. The FDM process was used to fabricate material testing samples for mechanical, electrical, and thermal properties investigation of the developed nanocomposites. The following highlights are made from the results of this study.

- i) There was an improvement of 11.6% tensile strength at 3wt% loading levels of CNF, however, 18.99% decrease of the tensile strength was observed when increasing the concentration of CNF to 5wt%. The agglomeration tendency of CNF is a well understood phenomenon and maximizing CNF potential at higher loading levels require optimizing the parameters of the manufacturing process.
- ii) Significant improvement of 86.9% increment in the tensile modulus was observed at the 3wt% CNF loading. However, no significant effect was observed in the tensile modulus of 5wt%. This could be due to a porous interfacial strength for effective load transfer. There was an improvement of Flexural properties with increasing CNF inclusion
- iii) The thermal properties of the nanocomposites were sustained with incorporation of CNF and no major deterioration was observed. No significant improvement in the thermal stability, weight percent loss, glass transition temperature of the nanocomposite. However, the crystallization transitions confirm higher degree of crystallinity with CNF inclusion.

- iv) Carbon Nanofiber has proved to improve the electrical properties by lowering the volume resistivity of the insulating Nylon matrix from the order 10^{13} to 10^{11} and 10^{12} for 3 and 5 wt.% respectively. The allowable electrical resistivity values for ESD compliance is rated between 10^{10} - 10^{12} ohms.cm, which makes the values observed at 3w.t% loading quite significant in this range and can be viable for electrostatic discharge application.
- v) It can be concluded from this study that the inclusion of CNF has shown high potential of developing a multifunctional PA6 nanocomposite for 3D printing. This was significant at 3wt% CNF addition which possess an excellent combination of mechanical, electrical, and thermal properties.

5.2 Recommendation

It is imperative to consider carrying out an extensive microstructural study via Transmission Electron Microscopy (TEM) to evaluate interfacial properties between the CNF and the Nylon matrix. TEM is a higher magnification studies which would be viable in understanding the interaction in surface properties of constituents' materials, especially at 5wt% where a decline in tensile properties values was observed.

APPENDIX SECTION

Appendix A: Technical Data Sheets (TDS)

	www.taulman3d.com	
	Specification	645 Nylon
Notes:	Technical	
1	Manufacture Part ID	tau51/tau53
	HS Code	3916.9
	Thermal	
2	Printing Temperature	250C-255C
	Melting Temperature	217C
3	Tg Glass transition	52C
4	Pyrolysis - Thermal degradation	340C
	Non-Destructive Evaluation	Yes
5	Print-Bed Temp	30-65C
6	Ambient Temp (Enclosure)	30 - 100C
	Physical	
	Nominal Diameter (3mm Maximum Dia)	1.75mm/2.85mm
	Weight /spool	1 lb
	Nominal Length/spool (In Feet)	490/180
7	Shrinkage - in/in	0.0062
8	Solvent/Glue	ComPlete
	Mechanical	
	Tensile Stress "PSI" when 3D Printed	5,188
	Ultimate Elongation when 3D Printed	186%
	Modulus "PSI" when 3D Printed	30,845
	Optical	
	Opacity	45%
	Reflectivity	N/A
10	Color	Natural
	Approvals	
	FDA - Direct Food Contact	None
	FDA Direct Drink Contact	None
	UL Flammability	
	UL 94 HB	Yes
	UL 94 V2 at 1.5 mm thickness	Yes

PR-24-XT-LHT Data Sheet

Product Nomenclature

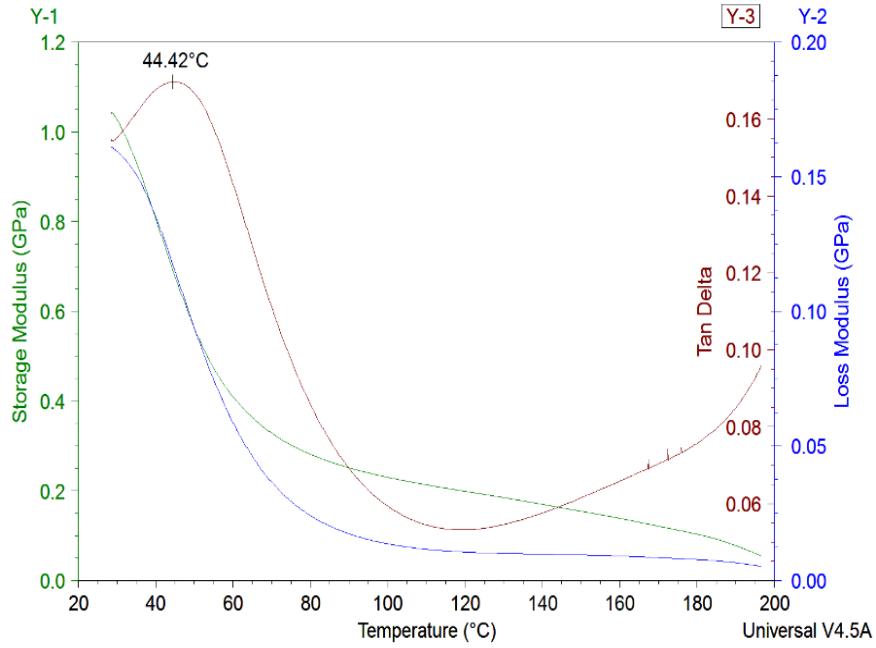
The LHT grade is produced by heat-treating the fiber at 1500°C. This converts any chemically vapor deposited carbon present on the surface of the fiber to a short range ordered structure. The inherent conductivity of the fiber is increased.

Carbon nanofiber properties

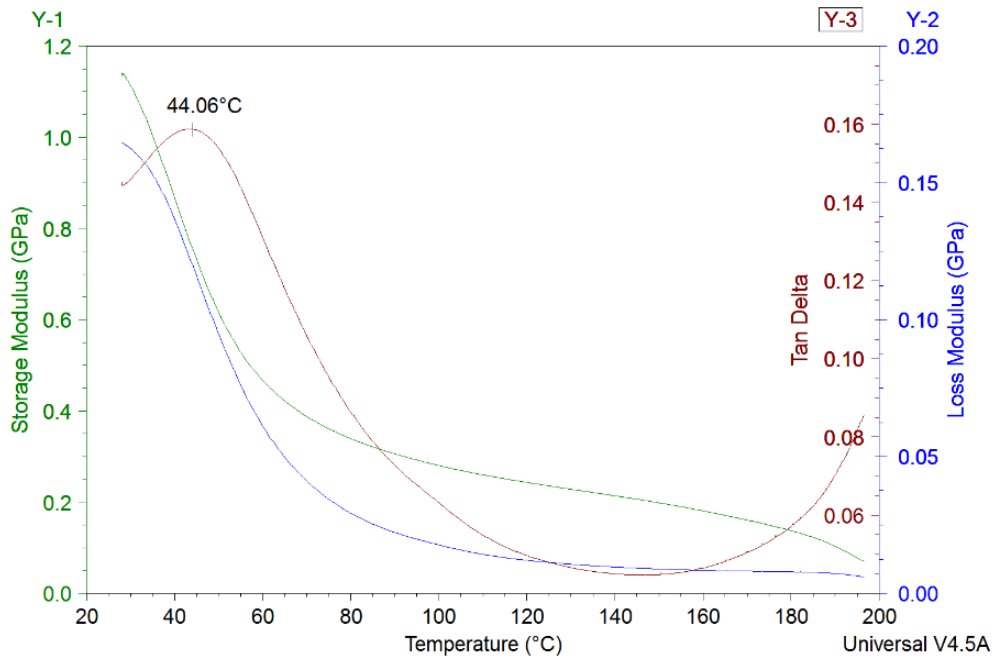
Fiber diameter, nm (average):	100
CVD carbon overcoat present on fiber:	no
Surface area, m ² /gm:	43
Dispersive surface energy, mJ/m ² :	155
Moisture, wt%:	<5
Iron, ppm:	<14,000
Polyaromatic hydrocarbons, mg PAH/gm fiber:	<1

Applications: Mechanical, and Electrical

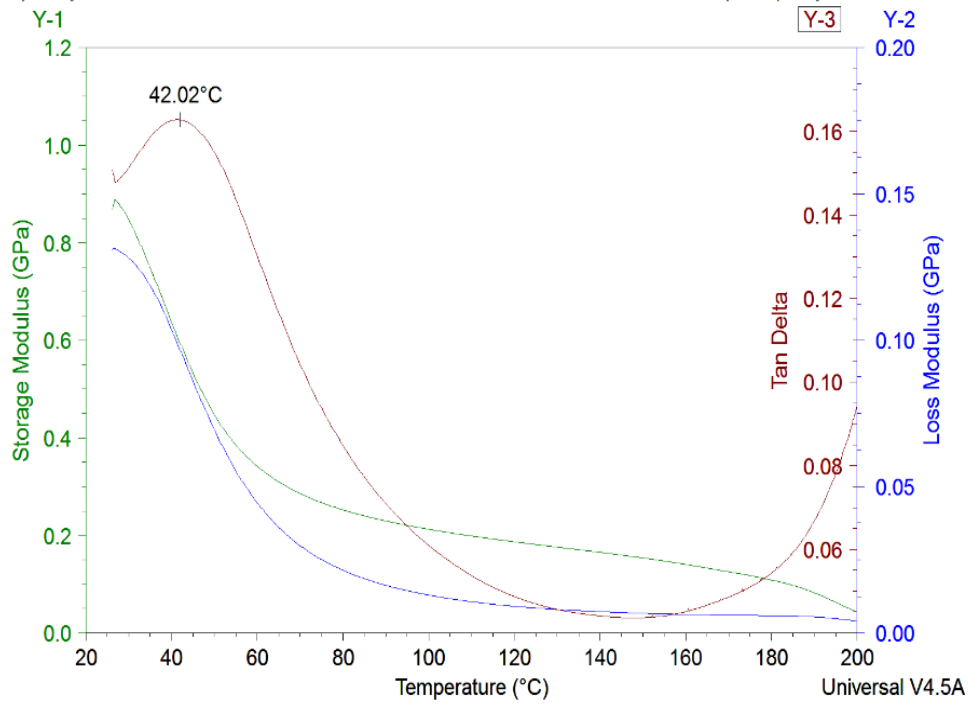
Appendix B: Superimposed DMA Thermograms



(a) DMA thermograms of 0wt. PA6/CNF Nanocomposite showing a superimposed storage modulus, loss modulus and tan delta



(b) DMA thermograms of 3wt.% PA6/CNF Nanocomposite showing a superimposed storage modulus, loss modulus and tan delta



(c) DMA thermograms of 5wt.% PA6/CNF Nanocomposite showing a superimposed storage modulus, loss modulus and tan delta

REFERENCES

- [1] P.-C. Ma, N. A. Siddiqui, G. Marom, and J.-K. Kim, "Dispersion and functionalization of carbon nanotubes for polymer-based nanocomposites: A review," *Composites Part A: Applied Science and Manufacturing*, vol. 41, no. 10, pp. 1345-1367, 2010/10/01/ 2010, doi: <https://doi.org/10.1016/j.compositesa.2010.07.003>.
- [2] "Introduction to ESD " Comchip Technology.
http://www.mouser.cn/pdfDocs/Comchip_ProductTraining_ESD20121023.pdf
(accessed).
- [3] "ESD material, ESD plastics." ROCHLING
<https://www.roechling.com/industrial/characteristics/esd-plastic/> (accessed).
- [4] S. Thermoplastics. "Polymer Electrical Conductivity."
https://www.starthermoplastics.com/2015/06/09/polymer_electrical_conductivity/
(accessed).
- [5] "Introducing FDM Nylon 6 – New 3D Printing Material." Cimquest Inc.
<https://cimquest-inc.com/introducing-fdm-nylon-6-new-3d-printing-material/>
(accessed).
- [6] X. Liu, R. Zhang, H. Zhu, and J. Wang, "Modeling method for battery distribution path optimization of EV charging and swapping service network," *Dianli Zidonghua Shebei/Electric Power Automation Equipment*, vol. 35, no. 6, pp. 10-16, 2015, doi: 10.16081/j.issn.1006-6047.2015.06.002.
- [7] T. D. Ngo, A. Kashani, G. Imbalzano, K. T. Q. Nguyen, and D. Hui, "Additive manufacturing (3D printing): A review of materials, methods, applications and challenges," *Composites Part B: Engineering*, vol. 143, pp. 172-196, 2018/06/15/ 2018, doi: <https://doi.org/10.1016/j.compositesb.2018.02.012>.
- [8] C.-C. Kuo *et al.*, "Preparation of starch/acrylonitrile-butadiene-styrene copolymers (ABS) biomass alloys and their feasible evaluation for 3D printing applications," *Composites Part B: Engineering*, vol. 86, pp. 36-39, 2016/02/01/ 2016, doi: <https://doi.org/10.1016/j.compositesb.2015.10.005>.
- [9] M. L. Shofner, K. Lozano, F. J. Rodríguez-Macías, and E. V. Barrera, "Nanofiber-reinforced polymers prepared by fused deposition modeling," *Journal of Applied Polymer Science*, vol. 89, no. 11, pp. 3081-3090, 2003, doi: 10.1002/app.12496.

- [10] K. S. Boparai, R. Singh, F. Fabbrocino, and F. Fraternali, "Thermal characterization of recycled polymer for additive manufacturing applications," *Composites Part B: Engineering*, vol. 106, pp. 42-47, 2016/12/01/ 2016, doi: <https://doi.org/10.1016/j.compositesb.2016.09.009>.
- [11] L. Zonder, A. Ophir, S. Kenig, and S. McCarthy, "The effect of carbon nanotubes on the rheology and electrical resistivity of polyamide 12/high density polyethylene blends," *Polymer*, vol. 52, no. 22, pp. 5085-5091, 2011/10/13/ 2011, doi: <https://doi.org/10.1016/j.polymer.2011.08.048>.
- [12] S. Gaikwad, J. Tate, N. Theodoropoulou, and J. Koo, "Electrical and mechanical properties of PA11 blended with nanographene platelets using industrial twin-screw extruder for selective laser sintering," *Journal of Composite Materials*, vol. 47, no. 23, pp. 2973-2986, 2013, doi: 10.1177/0021998312460560.
- [13] A.-C. Brosse, S. Tencé-Girault, P. M. Piccione, and L. Leibler, "Effect of multi-walled carbon nanotubes on the lamellae morphology of polyamide-6," *Polymer*, vol. 49, no. 21, pp. 4680-4686, 2008/10/06/ 2008, doi: <https://doi.org/10.1016/j.polymer.2008.08.003>.
- [14] R. Chávez-Medellín, L. A. S. d. A. Prado, and K. Schulte, "Polyamide-12/Functionalized Carbon Nanofiber Composites: Evaluation of Thermal and Mechanical Properties," *Macromolecular Materials and Engineering*, vol. 295, no. 4, pp. 397-405, 2010, doi: 10.1002/mame.200900316.
- [15] W. Chanklin, "Electrical Properties Study of Carbon Fillers in Polymer Nanocomposites " Doctor of Philosophy Chemical Engineering, The University of New Brunswick, New Brunswick, Canada, 2016. [Online]. Available: <https://pdfs.semanticscholar.org/fe28/6556c855aa21cddc41b79c8edcce142ab002.pdf>
- [16] A. Allaoui, S. V. Hoa, and M. D. Pugh, "The electronic transport properties and microstructure of carbon nanofiber/epoxy composites," *Composites Science and Technology*, vol. 68, no. 2, pp. 410-416, 2008/02/01/ 2008, doi: <https://doi.org/10.1016/j.compscitech.2007.06.028>.
- [17] F. K. Ko and Y. Wan, *Introduction to Nanofiber Materials*. Cambridge: Cambridge University Press, 2014.
- [18] "Pyrograf III." http://pyrografproducts.com/Merchant5/merchant.mvc?Screen=cp_nanofiber (accessed).
- [19] S. Fu, Z. Sun, P. Huang, Y. Li, and N. Hu, "Some basic aspects of polymer nanocomposites: A critical review," *Nano Materials Science*, vol. 1, no. 1, pp. 2-30, 2019/03/01/ 2019, doi: <https://doi.org/10.1016/j.nanoms.2019.02.006>.

- [20] H. v. K. Kohlgrüber. Co-Rotating Twin-Screw Extruder [Online] Available: http://files.hanser.de/Files/Article/ARTK_LPR_9783446413726_0001.pdf
- [21] H. K. Reimschuessel, "Polyamides," in *Encyclopedia of Materials: Science and Technology*, K. H. J. Buschow *et al.* Eds. Oxford: Elsevier, 2001, pp. 7147-7149.
- [22] S. Kundu, P. Jana, D. De, and M. Roy, "SEM image processing of polymer nanocomposites to estimate filler content," in *2015 IEEE International Conference on Electrical, Computer and Communication Technologies (ICECCT)*, 5-7 March 2015 2015, pp. 1-5, doi: 10.1109/ICECCT.2015.7226104.
- [23] ASTM. "Standard Test Method for Tensile Properties of Plastics." <https://www.astm.org/Standards/D638.htm> (accessed).
- [24] A. S. D790, " " Standard Test Methods for Flexural Properties of Unreinforced and Reinforced Plastics and Electrical Insulating Materials," ASTM International, West Conshohocken, PA," 2010.
- [25] ASTM. "Standard Test Methods for DC Resistance or Conductance of Insulating Materials." <https://www.astm.org/Standards/D257.htm> (accessed).
- [26] ASTM. "Standard Test Method for Thermal Stability by Thermogravimetry." <https://www.astm.org/Standards/E2550.htm> (accessed).
- [27] ASTM. "Standard Test Method for Transition Temperatures and Enthalpies of Fusion and Crystallization of Polymers by Differential Scanning Calorimetry." <https://www.astm.org/Standards/D3418.htm> (accessed).
- [28] ASTM, "Standard Practice for Plastics: Dynamic Mechanical Properties: Determination and Report of Procedures " 2012. [Online]. Available: <https://www.astm.org/Standards/D4065.htm>.
- [29] G. Sui, W.-H. Zhong, M. A. Fuqua, and C. A. Ulven, "Crystalline Structure and Properties of Carbon Nanofiber Composites Prepared by Melt Extrusion," *Macromolecular Chemistry and Physics*, vol. 208, no. 17, pp. 1928-1936, 2007, doi: 10.1002/macp.200700170.
- [30] N. Mahmood, M. Islam, A. Hameed, S. Saeed, and A. N. Khan, "Polyamide-6-based composites reinforced with pristine or functionalized multi-walled carbon nanotubes produced using melt extrusion technique," *Journal of Composite Materials*, vol. 48, no. 10, pp. 1197-1207, 2014, doi: 10.1177/0021998313484779.

- [31] S. Y. Veena Choudhary and Anju Gupta , IntechOpen, . , "Polymer/Carbon Nanotube Nanocomposites, Carbon Nanotubes - Polymer Nanocomposites," 2011.
- [32] L. Feng, N. Xie, and J. Zhong, "Carbon Nanofibers and Their Composites: A Review of Synthesizing, Properties and Applications," (in eng), *Materials (Basel)*, vol. 7, no. 5, pp. 3919-3945, 2014, doi: 10.3390/ma7053919.
- [33] G. G. Tibbetts, I. C. Finegan, and C. Kwag, "Mechanical and electrical properties of vapor-grown carbon fiber thermoplastic composites," *Molecular Crystals and Liquid Crystals*, vol. 387, no. 1, pp. 129-133, 2002/01/01 2002, doi: 10.1080/10587250215229.
- [34] A. K. Barick and D. K. Tripathy, "Preparation and characterization of carbon nanofiber reinforced thermoplastic polyurethane nanocomposites," *Journal of Applied Polymer Science*, vol. 124, no. 1, pp. 765-780, 2012, doi: 10.1002/app.35066.
- [35] T. H. Courtney, *Mechanical Behavior of Materials*, Second Edition ed. Waveland press, Inc, 2000.
- [36] G. W. Ehrenstein and R. P. Theriault, *Polymeric materials : structure, properties, applications*. Munich; Cincinnati, OH: Hanser ; Hanser Gardner Publications (in English), 2001.
- [37] S. Z. D. Cheng and B. Lotz, "Enthalpic and entropic origins of nucleation barriers during polymer crystallization: the Hoffman–Lauritzen theory and beyond," *Polymer*, vol. 46, no. 20, pp. 8662-8681, 2005/09/23/ 2005, doi: <https://doi.org/10.1016/j.polymer.2005.03.125>.
- [38] C. Millot, L.-A. Fillot, O. Lame, and P. Sotta, "Assessment of polyamide-6 crystallinity by DSC: Temperature dependence of the melting enthalpy," *Journal of Thermal Analysis and Calorimetry*, vol. 122, 04/09 2015, doi: 10.1007/s10973-015-4670-5.
- [39] A. Eitan, F. T. Fisher, R. Andrews, L. C. Brinson, and L. S. Schadler, "Reinforcement mechanisms in MWCNT-filled polycarbonate," *Composites Science and Technology*, vol. 66, no. 9, pp. 1162-1173, 2006/07/01/ 2006, doi: <https://doi.org/10.1016/j.compscitech.2005.10.004>.
- [40] S. Yang, J. Taha-Tijerina, V. Serrato-Diaz, K. Hernandez, and K. Lozano, "Dynamic mechanical and thermal analysis of aligned vapor grown carbon nanofiber reinforced polyethylene," *Composites Part B: Engineering*, vol. 38, no. 2, pp. 228-235, 2007/03/01/ 2007, doi: <https://doi.org/10.1016/j.compositesb.2006.04.003>.